Coordination Chemistry Reviews 255 (2011) 2426–2447

Contents lists available at ScienceDirect

Coordination Chemistry Reviews

journal homepage: www.elsevier.com/locate/ccr

Review

Heteropolynuclear cycloplatinated complexes: Structural and photophysical properties

Álvaro Díez, Elena Lalinde*, M. Teresa Moreno*

Departamento de Química-Grupo de Síntesis Química de La Rioja, UA-CSIC, Universidad de La Rioja, 26006 Logroño, Spain

Contents

ARTICLE INFO

Article history:
Received 28 September 2010
Accepted 30 December 2010
Available online 11 January 2011

Keywords:
Cyclometalated ligands
Luminescence
Platinum
Polynuclear complexes

ABSTRACT

Cyclometalated Pt^{II} complexes have drawn a lot of interest because they show interesting photoluminescence properties with potential applications in optical materials such as OLEDs and WOLEDs. Recently, heteropolymetallic cycloplatinated complexes have also been identified as systems of interest because they readily allow emission tuning by suitable choice of heterometal, cyclometalated groups and coligands. This review describes the synthetic routes, structural aspects and photoluminescence properties of heteropolynuclear complexes containing cycloplatinated fragments. In turn, cycloplatinated complexes have also been investigated as molecular sensors of ions via photoluminescence responses.

1. Introduction

Square-planar cycloplatinated complexes have been extensively investigated in recent years due to their unique photophysical properties [1–8]. Apart from the fundamental interest in their intrinsic emissive states, these compounds are potentially useful for optical materials such as light-emitting devices [2,3,8–14], photocatalysts [15], photochemical sensors and biological labeling probes [16–19].

In these complexes, a typical emitting state might exhibit ligand-centered (^{3}LC) character and/or metal-to-ligand charge transfer (^{3}MLCT) character, although emissive states involving some degree of ligand-to-ligand′ charge transfer (^{3}LL′CT) are also possible. In addition, the absence of axial ligands in Pt^{II} complexes plays a key role in shaping other intriguing spectroscopic and photophysical properties, associated with the formation of dimers or extended networks controlled by non-covalent π···π and/or Pt···Pt interplanar stacking interactions, accessible not only in solid state but also in solution [20–30]. As a result, the associated phosphorescence is more or less red-shifted in relation to isolated monomers being derived from ^{3}ππ and/or metal–metal-to-ligand charge transfer (^{3}MMLCT) excited states.

In this area, considerable efforts have been devoted to the study of mononuclear Pt^{II} complexes and more recently also to di and trinuclear platinum derivatives [31–44], in which excited-state

Abbreviations: 18-crown-6, 1,4,7,10,13,16-hexaoxacyclooctadecane; acac, 2,4-pentanedionate; bpy, 2,2′-bipyridine; bzq, 7,8-benzoquinolate; cyclen, 1,4,7,10-tetraazacyclododecane; dppf, 1,1′-bis(diphenylphosphino)ferrocene; dppm, bis(diphenylphosphino)methane; dppy, 2-diphenylphosphinopyridine; Hdmpz, dimethylpyrazol; HOMO, highest occupied molecular orbital; Hppy, 2-phenylpyridine; Hthpy, 2-(2-thienyl)pyridine; Hphbpy, 6-phenyl-2,2′-bipyridine; HppyFF, 2-(2,4-difluorophenylpyridine); LUMO, lowest unoccupied molecular orbital; P_2Phen, 2,9-bis(diphenylphosphine)-1,10-phenantroline; pz, pyrazol; TD-DFT, time-dependent density functional theory.

* Corresponding authors. Fax: +34 941 299 621.
E-mail addresses: elena.lalinde@unirioja.es (E. Lalinde), teresa.moreno@unirioja.es (M.T. Moreno).

0010-8545/$ – see front matter © 2011 Elsevier B.V. All rights reserved.
doi:10.1016/j.ccr.2010.12.024

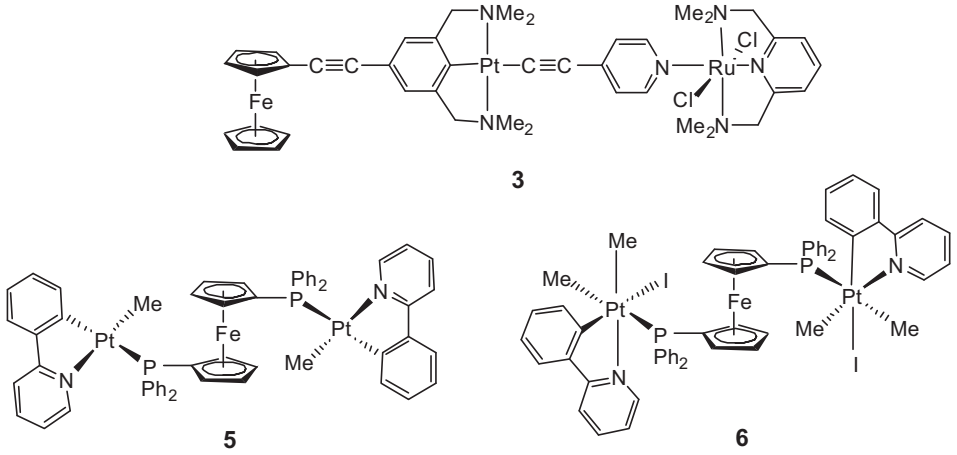

Chart 1.

properties or even the nature of the emissive state can be tuned (or modified) through structural modifications on the cyclometalated group and coligands or by tailoring the characteristics of the bridging units. These properties, together with high quantum yields and thermal stability, have made them of particular interest in OLEDs [34,37]. In addition, the propensity to form excimers or aggregates, which is not usually associated with the d^6 (Re^I, Os^{II}, Ir^{III}) family of emitters, provides an interesting alternative for obtaining single-layer white organic light emitting diodes (WOLEDs) [45], which has stimulated the work in this field. In this area, excellent reviews dealing with different aspects of square-planar platinum complexes have been published [1–11,46–52].

On the other hand, the study of heteropolynuclear aggregates containing closed shell (d^{10}, d^8, d^{10} s^2) metal ions has increased considerably, in part because of their unique luminescent properties, which in some cases have been attributed to the presence of metallophilic bonds [53–62]. Moreover, metallophilic bonding interactions have also been recognized as a powerful tool in molecular or crystal engineering [63]. In this field, electron rich Pt^{II} complexes have been widely employed [53–56], though the number of heterometallic assemblies based on cycloplatinated units are still scarce. It should be noted that the electron-donor properties of the platinum(II) complexes containing cyclometalated ligands can improve their ability to form Pt → M donor–acceptor bonds. The molecular orbitals scheme for this type of donor–acceptor bonds [64,65] indicates that when the Pt^{II} is located in a strong ligand field, such as that exerted by cyclometalated ligands, a stronger dative bond will be formed employing the occupied higher-energy $d_z{}^2$ on Pt^{II} as donor orbital.

Although different aspects including photophysical properties of a wide range of heteropolymetallic systems have been reviewed [53–62], as far as we know, no review article involving heteropolymetallic cycloplatinated complexes has been reported. Therefore, this contribution is confined to synthetic, structural and electronic properties of heteropolynuclear and/or multicomponent complexes incorporating cycloplatinated fragments, with particular attention to emissive systems and also including the photoresponse of some of them towards different metal ions, which have been utilized as molecular switches or sensors of ions.

2. Heterometallic transition metal complexes

2.1. Heteronuclear platinum-group 8–10 metal complexes

Ferrocene-based cycloplatinated systems have been widely described. Among them, examples of cycloplatinated compounds containing [C(sp^2,ferrocene), N]$^-$ bidentate [66–72] or [C(sp^2,ferrocene), N, X]$^-$ (X = N, S) terdentate [73–76] groups have been reported, some of them of particular relevance due to its antitumoral activity [71,72].

Heterobimetallic Fc–C≡C–NˆCˆN–Pt–C≡CR [Fc = (η^5-C_5H_5)(η^5-C_5H_4)Fe; NˆCˆN = [1,4-$C_6H_2(CH_2NMe_2)_2$-2,6]$^-$; R = bpy **1**, C_5H_4N-4 **2**] complexes are accessible by the methathesis of Fc–C≡C–NˆCˆN–PtCl with LiC≡CR [77]. The complexation of **2** with [Ru]N≡N[Ru] ([Ru] = [η^3-*mer*-{2,6-(Me_2NCH_2)$_2$$C_5H_3$N}$RuCl_2$]) occurs with liberation of N_2 to give the heterotrimetallic derivative **3** (Chart 1), in which the N-atom of the pendant pyridine unit coordinates to a [*mer*, *trans*-(*NN′N*)$RuCl_2$] complex fragment. The electronic influence of the metal units on each other has been demonstrated by cyclic voltammetry [77]. However, van Koten et al. have shown that coordination of this Ru-containing complex [Ru] to the nitrile function of the related unsubstituted platinum complex {Pt}(C≡C–C_6H_5–CN-4) ({Pt} = Pt(C_6H_3{Me_2NCH_2}$_2$-2,6) in complex {Pt}C≡C–C_6H_5–CN-4[Ru] **4** does not alter the electrochemical properties of the Pt core [78]. Also, no influence of the Pt on the electrochemical behavior of the Ru complex fragment was observed [79].

1,1′-Bis(diphenylphosphino)ferrocene (dppf) acts as a bidentate ligand connecting two cyclometalated organoplatinum(II) species, containing a deprotonated ppy ligand, in [Pt_2Me_2(ppy)$_2$(μ-dppf)] **5** [80] (Chart 1). The platinum(II) centers in this complex undergo oxidative addition of MeI to give the corresponding Pt^{IV}–Pt^{IV} complex [$Pt_2I_2Me_4$(ppy)$_2$(μ-dppf)] **6**. The mechanism for this reaction was established on the basis of NMR and UV–vis spectroscopic studies.

Pt^{II}-bis(dicobaltotetrahedrane) adducts [{(μ-η^2-NˆCˆN)Pt(η^1-CO) (C≡CSiMe_3)}{$Co_2(CO)_6$}] [79] **7** and [(μ-Me_3SiC≡C){Pt}Cl{$Co_2(CO)_6$}] **8** ({Pt} = Pt(C_6H_2-{CH_2NMe_2}$_2$-2,6) [78] have

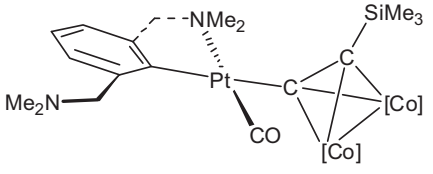

7

[Co] = $Co(CO)_3$

Chart 2.

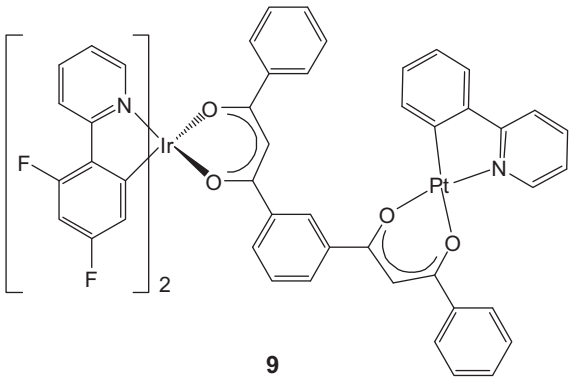

9

Chart 3.

been obtained by reaction of [Pt(R-NˆCˆN)(C≡CSiMe$_3$)] (R = H, C≡CSiMe$_3$; NˆCˆN = 1,4-C$_6$H$_2$-{CH$_2$NMe$_2$}$_2$-2,6) with [Co$_2$(CO)$_8$] (Chart 2), via η^2-coordination to the corresponding alkyne or alkynyl unit. In complex **7**, an incoming CO ligand has displaced one *o*-CH$_2$NMe$_2$ substituent to form the CˆN chelate bidentate ligand [79].

A Pt^{II}–Ir^{III} heterobinuclear complex linked by a bis(β-diketonato) bridging ligand [{Ir(ppyFF)$_2$}(μ-L){Pt(ppy)}] **9** [H$_2$L = 1,3-bis(3-phenyl-3-oxo-propanoyl)benzene] has been recently described (Chart 3) [81]. Single crystal X-ray data suggest the possibility of Ir···Pt electronic interaction through the bridging ligand (O–M–O units/phenylene dihedral angles 18.74°, 10.68°) and reveal the presence of extensive intermolecular π···π stacking interactions involving both metal moieties [Ir(ppyFF)···(ppyFF)Ir, Pt(ppy)···(ppy)Pt; PtL···PtL].

The UV–vis spectrum of **9** shows the typical metal-to-ligand charge transfer low-energy features corresponding to the sum of the independent absorption spectra of both metal units, indicating that the electronic transition at each metal unit is not affected by the bis(β-diketonato) bridging ligand. However, **9** exhibits an emission band in degassed CHCl$_3$ solution both at 298 K (λ_{max} 615 nm, τ = 22 ns; ϕ = 0.023) and at 77 K (λ_{max} 570 nm, τ = 1.4 μs), dominated by the L-based triplet excited state (^{3}LX), reflecting the occurrence of an efficient energy convergence from the triplet states of the Pt(ppy) and Ir(ppyFF) units to the lowest-lying ^{3}LX state of L bridging ligand. Interestingly, an intense orange-red emission (λ_{max} = 597 nm, τ = 0.56 ns) is observed in solid state at 298 K, which is ascribed to aggregation-induced (AIE) ^{3}M(LL)CT emission, associated with the strong π···π intermolecular interactions between adjacent pyridine rings of ppyFF ligands at the Ir^{III} units. The electrochemical properties of **9** indicate that the first two reductions occur at the L bridging ligand, which supports evidence that the L bridging ligand dominates the lowest excited state in solution.

Double deprotonation of *cis*-[Pt(C≡CPh)$_2$(Hdmpz)$_2$] with [M(CˆP)(μ-O$_2$CCH$_3$)]$_2$ [M = Pd, Pt; CˆP = CH$_2$-C$_6$H$_4$-P(*o*-tolyl)$_2$-κ*C*,*P*] in the presence of NEt$_3$ affords the trinuclear complexes [Pt(μ-C≡CPh)$_2$(μ-dmpz)$_2${M(CˆP)}$_2$] (M = Pd, Pt) (**10**, Chart 4), which do not show emissive properties [82]. The dianionic ligand [C$_6$(CH$_2$-NMe$_2$)$_4$-2,3,5,6]$^{2-}$ acts as aromatic spacer between a Pt^{II} and a Pd^{II} center with two NˆCˆN coordination moieties, giving the heterobinuclear Pt^{II}–Pd^{II} derivatives [(LPd)-1-(PtL)-4-{C$_6$(CH$_2$NMe$_2$)$_4$-2,3,5,6}]$^{n+}$(X$^-$)$_2$ (L = Cl, X = no anion; L = MeCN, X = OTf, BF$_4$) [83] (**11**, Chart 4), which have potential for electronic M–M′ communication and could be employed as building blocks for extended materials by exchange of the labile ligands (Cl, NCMe).

Recently, Osuka, Shinokubo et al. have introduced cyclometalation strategies to prepare unusual transition metal porphyrin complexes that have a carbon–metal σ-bond at the peripheral porphyrin. An interesting route is to use coordinating substituents such as pyridyl groups at the β-positions adjacent to the unsubstituted *meso*-position of 5,10,15-triarylporphyrins, which accommodate a variety of metals in the central cavity. Thus, the reaction of β-pyridyl nickel porphyrins with K$_2$PtCl$_4$ at 100 °C in toluene/DMF solution gives rise to an unusual DMF–Pt^{IV}–nickel porphyrin complex bearing sp^2 C-Pt and sp^3 C-Pt bonds in a *cis* configuration (**12-Ni**, Scheme 1) [84]. From the reaction mixture, a Pt^{II}–CO complex was also isolated (**13**, Scheme 1). When the reaction was carried out in the presence of NaOAc as a proton scavenger, a simultaneous C–H bond double activation also occurred affording the DMF-appended Pt^{II} porphyrin **14-Ni**. This procedure was nicely extended to Zn and Cu porphyrins (**14-M**). The electronic spectra of complexes **12-M** and **14-M** are red shifted with respect to those of the monomeric porphyrin precursors (*i.e.* Δ = 1825 cm^{-1} **14-Ni**, 1378 cm^{-1} **12-Ni** for the Q bands), which have been attributed to expansion of conjugation by the forced coplanarity of the pyridyl group and the porphyrin core.

Along the same lines, the reaction of the same nickel-porphyrin precursor with (NBu$_4$)$_2$PtCl$_6$ in toluene/AcOH provided a Pt^{IV}-bridged cofacial diporphyrin **15**, which can be successfully reduced with MeNHNH$_2$ in CH$_2$Cl$_2$ to give the analogous cofacial Pt^{II}-dimer **16** [85], via a formal "slipping motion" of the two porphyrin macrocycles, as confirmed by X-ray diffraction (Fig. 1). The platinum center forces the porphyrin macrocycles to be in close proximity (3.4-3.8 Å in **15**) and their electronic spectra broaden and split due to exciton coupling. A higher red shift of both the soret (Δ 825 cm^{-1}) and the Q-band was observed for the Pt^{II} complex **16** (Fig. 2), reflecting the importance of the higher electron donating ability of the Pt^{II} center, which raises the HOMO energy, as confirmed by DFT calculations. Electrochemical behavior of these Pt-bridged cofacial diporphyrins was also examined.

Other synthetic strategy to induce cyclometalation is to use appropriately selected inverted porphyrins. These precursors possess the external nitrogen of the inverted pyrrole, which can act as a donor site. Thus, reaction of 21-C-methyl and 21-C-benzyl nickel(II) complexes of inverted *meso*-tetrakis(*p*-tolyl)porphyrin with PtCl$_2$ or [PtCl$_2$(NCPh)$_2$] in refluxing CHCl$_3$ in the presence of K$_2$CO$_3$ yields *chemo* and *diastereoselectively* the chloroplatinum(II) species (**17**, Scheme 2) containing two nickel(II) carbaporphyrinoids in a *cis*

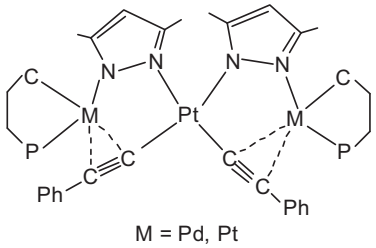

10

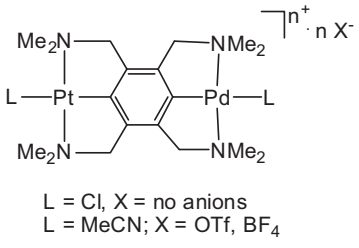

11

Chart 4.

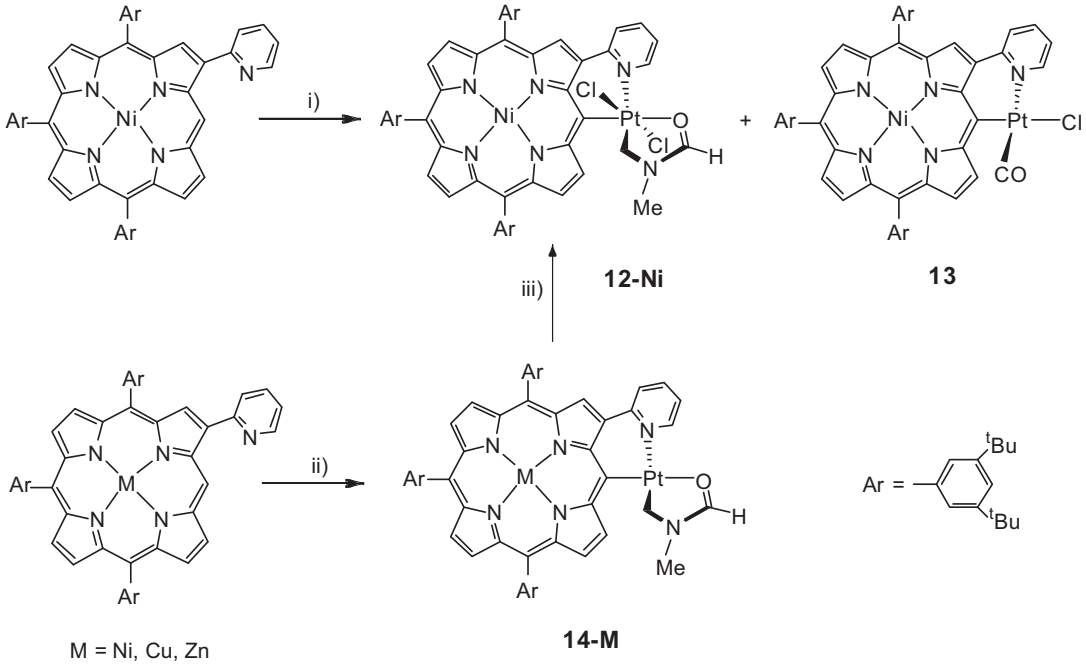

Scheme 1.

arrangement (SR, RS enantiomers), as confirmed by X-ray and NMR (^{1}H, ^{13}C) studies [86]. One of the carbaporphyrinoids coordinates to the Pt^{II} ion with the external nitrogen, whereas the other is bound with the external nitrogen and one *ortho*-carbon of the adjacent *meso*-aryl ring. In these systems, although electrochemical measurements reveal an anodic shift of the Ni^{II} oxidation potentials of **17** with respect to those of the parent precursors, their electronic spectra suggest little change in the electronic structure of the porphyrines upon metalation to Pt^{II}.

2.2. Heteronuclear platinum-group 11 (Cu, Ag, Au) metal complexes

As noted in the Introduction, Pt → M (M = Cu, Ag, Au) bonds play an important role in the synthesis of metal clusters [87] or extended supramolecular systems [88–90]. Some of these Pt–M systems have been found to display luminescent properties, which have been invariably related to the formation of the Pt–M bonds [53,90–96]. Recently, even a self-assembled luminescent octanuclear stellate platinacycle has been constructed via Pt–Ag dative bonds [97]. In this area, several cyclometalated platinum(II) complexes have been synthesized, and in some cases the influence of the Pt–M dative bonds on their physical properties has been studied.

Yamaguchi et al. [98] reported an interesting one-dimensional metal chain and a linear pentanuclear complex built from unsupported Pt → Ag bonds, using [Pt(ppy)$_2$] and [Pt(thpy)$_2$] as building templates. The cation structure in $[\{Pt(ppy)_2\}_2\{Ag(acetone)\}_2]_n(ClO_4)_{2n}\cdot nCH_3COCH_3$ **18**, obtained by slow evaporation of an acetone solution of [Pt(ppy)$_2$] and $AgClO_4$ (1:1), is a helical cationic chain constructed from alternating "Pt(ppy)$_2$" and "Ag(acetone)" units connected by Pt → Ag bonds [2.6781(9)–2.8121(9) Å] and stabilized by additional short π···π stacking contacts between the ppy ligands (~3.5 Å) (Fig. 3). Although the short Pt–Ag distances point to a significant donation from the d_z^2(Pt) orbital to the Ag^I cation, the Pt–Ag vector displaces from the perpendicular (24.8°) towards the metalated carbon atoms, allowing close Ag···C(π) contacts [2.364(10)–2.536(9) Å]. Considering the two Pt–C(metalate) bonds as formal donors, the silver ion is in a trigonal environment, which is completed by the acetone solvent.

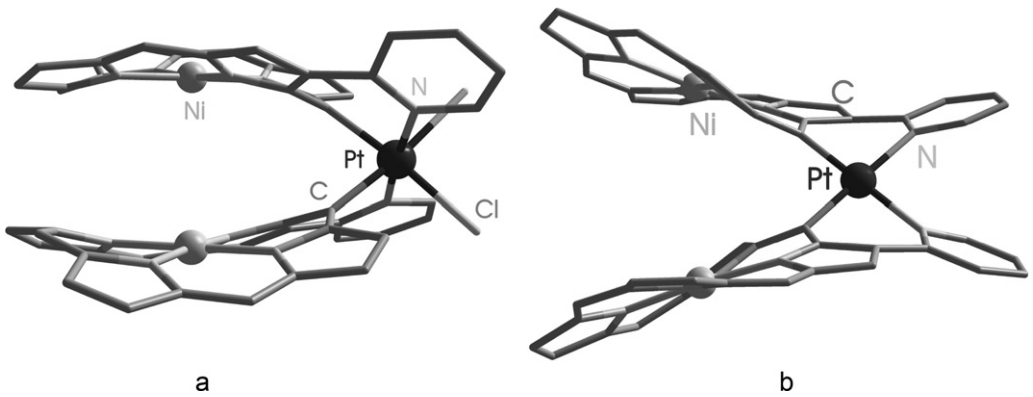

Fig. 1. Side views of the structures of the cofacial diporphyrins: (a) **15** and (b) **16**.

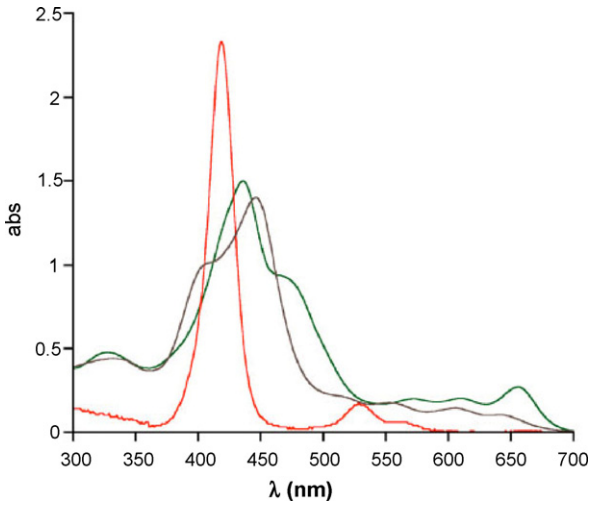

Fig. 2. UV–vis spectra of **15** (brown line), **16** (green line) and monomeric Ni-porphyrin precursor (red line).
Reprinted with permission of Ref. [85]. Copyright 2010. American Chemical Society (abs: $\varepsilon/10^{-5}\ M^{-1}\ cm^{-1}$).

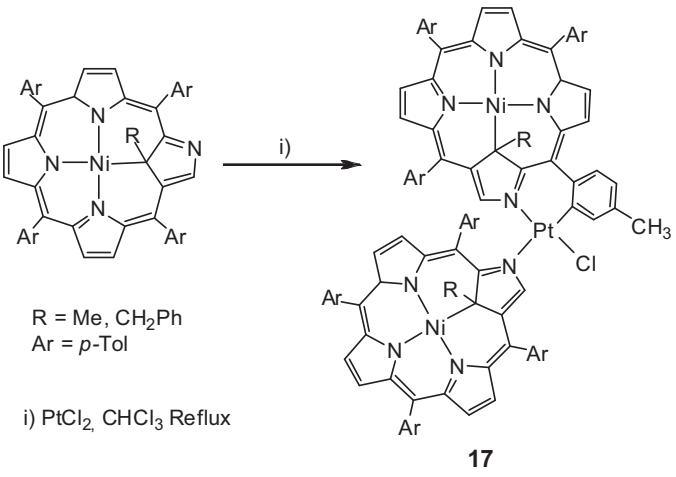

Scheme 2.

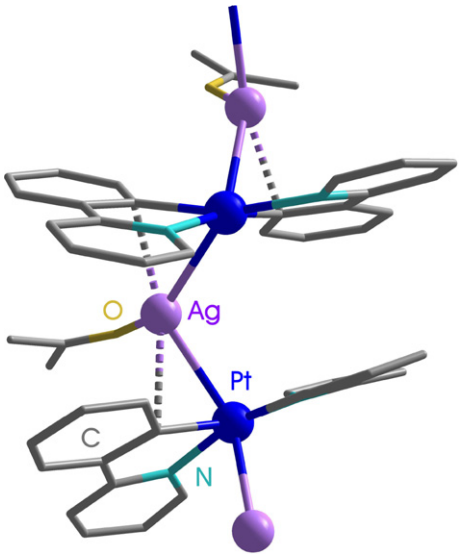

Fig. 3. Molecular structure of $[\{Pt(ppy)_2\}_2\{Ag(acetone)\}_2]_n^{2n+}$ in **18**.

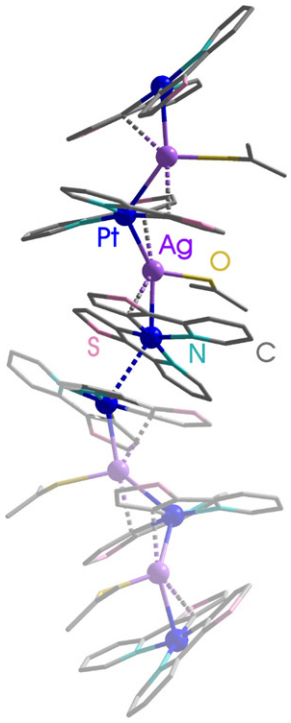

Fig. 4. Molecular structure of $[\{Pt(thpy)_2\}_3\{Ag(acetone)\}_2]^{2+}$ in **19**.

It is remarkable that similar reaction of $[Pt(thpy)_2]$ with Ag^I afforded the discrete linear pentanuclear complex $[\{Pt(thpy)_2\}_3\{Ag(acetone)\}_2](ClO_4)_2{\cdot}CH_3COCH_3$ **19** (Fig. 4). Structural details of the cation are similar to those of **18** [Pt–Ag 2.6746(7)–2.8083(6) Å; Ag–C_π 2.438(7)–2.558(7) Å], but in this case the chain ends at Pt sites, giving a final Pt–Ag–Pt–Ag–Pt pentanuclear cluster. Interestingly, the crystal packing of **19** reveals that the pentanuclear clusters are additionally assembled by weak Pt···Pt stacking interactions [Pt···Pt 3.2787(4) Å] giving rise to a 1-D chain. This fact seems to suggest that in these systems based on cycloplatinate fragments the well-known Pt···Pt stacking interactions [20–22,25–27,29,30] compete with the attractive $d^8\cdots d^{10}$ heterometallic Pt → Ag bonds and that they probably also play a significant role in the final stoichiometry. No luminescence studies are reported.

Another structure with completely unsupported Pt → Ag dative bonds appears in the trinuclear cluster $[\{Pt(ppy)(9S3)\}_2Ag(CH_3CN)_2](PF_6)_3$ **20** (9S3 = 1,4,7-trithiacyclononane), generated by incomplete dechlorination in the reaction system $[Pt(ppy)(\mu\text{-}Cl)]_2/AgPF_6/9S3$ (1:2:1) [99] (Fig. 5). The silver ion is bonded to two monocationic cyclometalated Pt^{II} units containing the tridentate thiacrown 9S3 ligand [2.7557(6), 2.7659(6) Å] and completes a distorted tetrahedral environment with two molecules of acetonitrile solvent. The formation of the Pt → Ag dative bonds causes a significant shortening of the axial Pt–S distance [2.6870(18), 2.7461(19) Å] in each Pt cationic unit (over 0.20 Å), when compared to that of the mononuclear complex $[Pt(ppy)(9S3)]PF_6$. By addition of an excess of $AgPF_6$ to a concentrated acetonitrile solution of $[Pt(ppy)(9S3)]PF_6$, a red shift of the low energy absorption feature (370–380 nm) was observed, but no photoluminescence studies were reported.

Our group has reported the synthesis, structural characterization and photophysical properties of three benzoquinolate species containing donor–acceptor Pt → Ag bonds [100]. Thus, neutralization reaction of $(NBu_4)[Pt(bzq)(C_6F_5)_2]$ with $AgClO_4$ in either 1:1 or 2:1 molar ratio evolved with formation of the trinuclear anionic complex $(NBu_4)[\{Pt(bzq)(C_6F_5)_2\}_2Ag]$ **21**, whereas the reaction

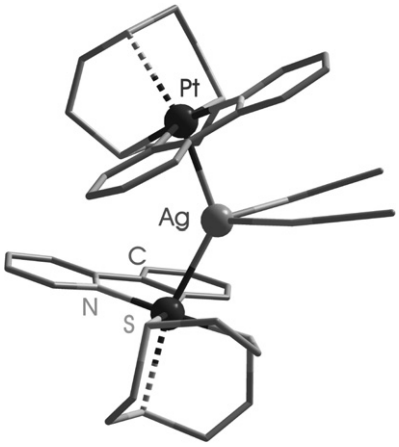

Fig. 5. Molecular structure of the cation $[\{Pt(ppy)(9S3)\}_2Ag(CH_3CN)_2]^{3+}$ in **20**.

of $(NBu_4)[Pt(bzq)(C_6X_5)_2]$ (X = F, Cl) with $[Ag(OClO_3)(PPh_3)]$ (1:1) afforded neutral bimetallic systems $[\{Pt(bzq)(C_6X_5)_2\}Ag(PPh_3)]$ (X = F **22**, Cl **23**). For complex **21**, two different polymorphs (monoclinic **21a** and triclinic **21b**, Fig. 6) were obtained from acetone/*n*-hexane. Both present a sandwich type structure with two square-planar "$Pt(bzq)(C_6F_5)_2$" units connected by a silver center. The electronic requirements of the dicoordinated Ag^I ion are fulfilled by the synergetic combination of two short Pt → Ag dative bonds and two Ag–C_π(metalate) bonding interactions, with the shorter Ag–C distances [Ag–C 2.420(6), 2.626(6) Å **21a**; 2.418(5), 2.538(5) Å **21b**] related to the longer Pt–Ag ones [Pt–Ag = 2.7584(5), 2.6843(5) **21a**; 2.7018(4), 2.6897(4) Å **21b**; Pt–Ag–Pt 136.49(2)° **21a**, 158.77(2)° **21b**]. Both polymorphs differ in the conformation of the platinum planes (*anti* and *planar* in **21a** and *staggered* and *non planar* in **21b**) and in the final packing of the anions in the lattice, which influences their optical properties (see below). In **21a**, the discrete anionic sandwiches interact by π···π (bzq) stacking interactions (~3.6 Å) to form an extended structure, whereas in **21b**, probably due to steric constraints, only a bzq ligand of each anion is involved in the stacking, giving rise to π-stacked dimers $(PtAgPt)_2$ (Fig. 6).

One striking feature in these structures (and also in the bimetallic neutral complexes **22** and **23**), which are based on heteroleptic pentafluorophenylcycloplatinate units, is the fact that no short *o*-F···Ag^I interactions are observed, a structural feature fairly common in many pentafluorophenylplatinate complexes with Pt → M (M = Ag^I, $Tl^{I,II}$, Pb^{II}, Sn^{II}) donor–acceptor bonds [87,101–105].

As shown in Fig. 7a and b, the Ag^I center in the neutral complexes **22** and **23** seems to avoid the steric repulsion caused by the C_6X_5 groups and again the Pt → Ag bonds are inclined towards the planar cyclometalated C(bzq) [34.9(1)° **22** and 27.2(1)° **23**]. A remarkable stronger Ag–C(π) interaction is observed in the C_6F_5 complex **22** [2.352(3) Å **22**, 2.557(5) Å **23**], which correlates with its longer Pt–Ag bond [2.7227(3) Å **22**, 2.6748(5) Å **23**]. The Ag^I center completes a formal dicoordination with a PPh_3 ligand, the Pt–Ag–P array being almost linear in **23** [145.24(3)° **22**, 173.53(4)° **23**]. Both complexes also form π-stacked dimers through bzq interactions, in a similar way to polymorph **21b**.

For cationic systems (**18**–**20**) the presence of the Pt–Ag bonds in solution is suggested by the occurrence of remarkable ^{195}Pt low-field shifts (~400 ppm **18**, **19**; 205 ppm **20**) upon the addition of

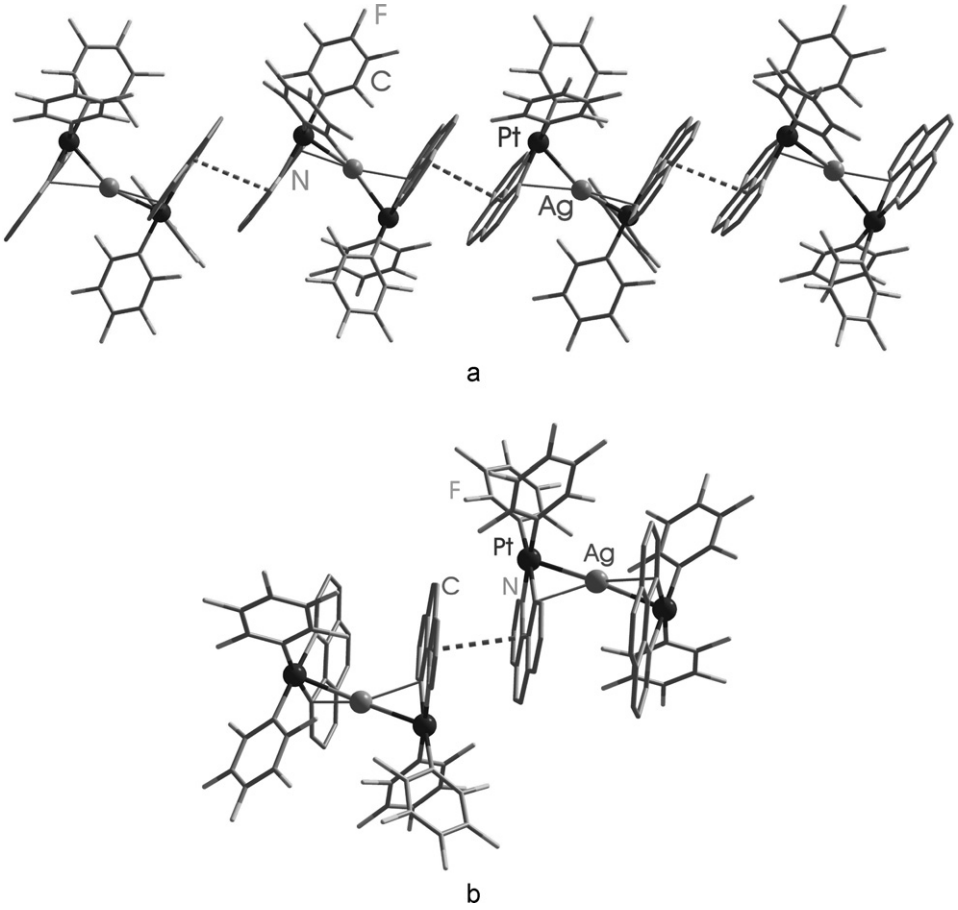

Fig. 6. Crystal packing of the anions of the two polymorphs of the complex $(NBu_4)[\{Pt(bzq)(C_6F_5)_2\}_2Ag]$: (a) monoclinic form **21a** and (b) triclinic form **21b**.

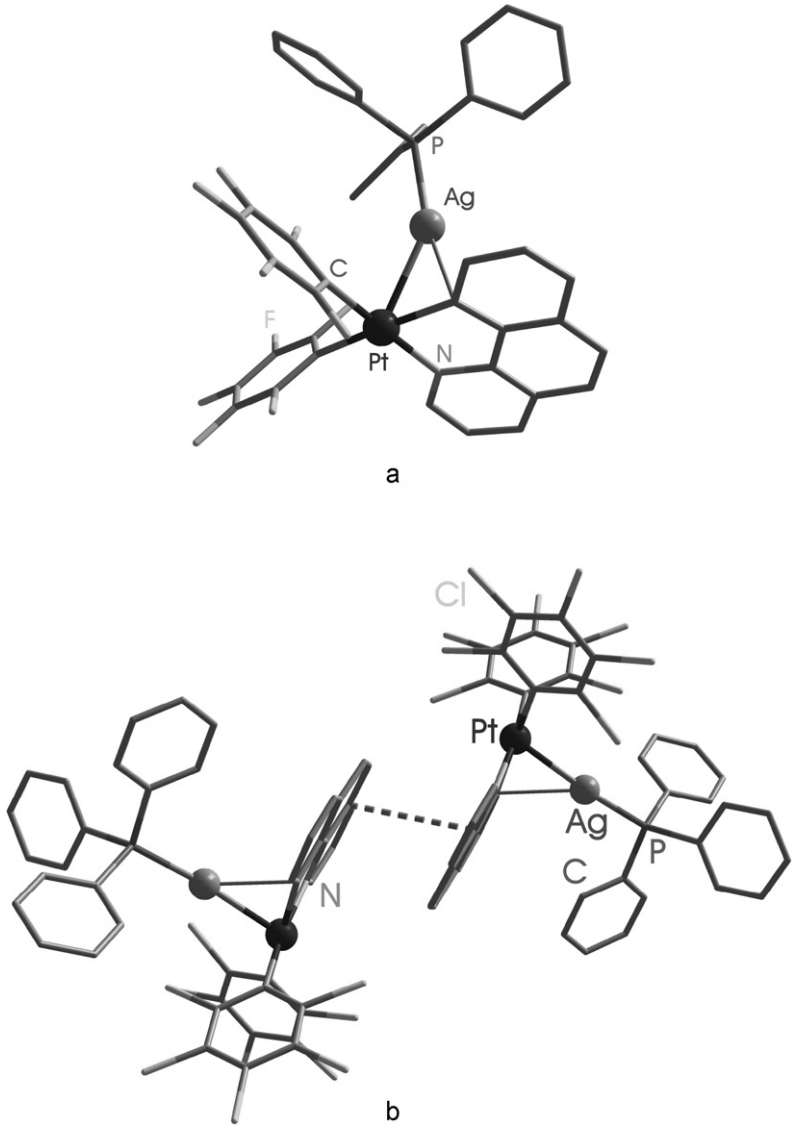

Fig. 7. View of the molecular structure of (a) [{Pt(bzq)(C_6F_5)$_2$}Ag(PPh_3)]·$CHCl_3$·0.5*n*-C_6H_4 (**22**·$CHCl_3$·0.5*n*-C_6H_4) and (b) [{Pt(bzq)(C_6Cl_5)$_2$}Ag(PPh_3)]·0.58$CHCl_3$·0.25*n*-C_6H_4 (**23**·0.58$CHCl_3$·0.25*n*-C_6H_4).

excess of Ag^I to the platinate precursors (δ ^{195}Pt–1928 [Pt(ppy)$_2$], −2204 [Pt(thpy)$_2$], −3787 [Pt(ppy)(9S3)](PF_6) [98,99]. This fact is in accordance with the expected decrease in the electron density of the Pt center upon bonding to Ag^I. However, complexes **18**–**20** appear to dissociate in solution. By contrast, the integrity of the neutral bimetallic complexes **22** and **23** in solution is retained, as is supported by $^{31}P\{^1H\}$ NMR and UV–vis spectroscopies. In both complexes (X = F **22**, Cl **23**) the doublet of doublet phosphorus signal due to ^{107}Ag, ^{109}Ag coupling also shows ^{195}Pt satellites ($^2J^{195}$Pt–P ∼ 230 Hz) confirming the persistence of the Pt–Ag bond in solution.

Along the same lines, the formation of the dative Pt → Ag bond, which increase the electrophilicity of the Pt center, lowers the energy of HOMO resulting in a blue shift of the low energy ^{1}MLCT absorption in the UV–vis spectra in relation to their precursors (CH_2Cl_2 413 nm **22** *vs.* [Pt(bzq)(C_6F_5)$_2$]$^-$ 425 nm; 420 nm **23** *vs.* [Pt(bzq)(C_6Cl_5)$_2$]$^-$ 444 nm). However, in the trinuclear anionic Pt_2Ag complex **21**, the electronic spectrum is similar to that of the precursor, indicating that its integrity is likely broken in solution.

At 298 K, in the solid state and in frozen CH_2Cl_2 solutions, both binuclear complexes **22** and **23** show an identical highly structured emission (λ_{max} 491 nm, τ = 12.4 μs **22**, 11.4 μs **23**), attributed to a ^{3}LC emissive state, with a negligible contribution of the Pt–Ag bond. However, upon cooling the solid at 77 K, two close structured emission bands with a short and long lifetime are resolved (**22**: λ 487 nm, τ = 12.4 μs; λ 502 nm, τ = 278 μs; **23**: λ 490 nm, τ = 21.2 μs; λ 502 nm, τ ∼ 206 μs) (Fig. 8). The structured low energy, which appears at 502 nm in both complexes, has been tentatively attributed to a $^3\pi\pi^*$ emissive state with intraligand character (^{3}LC). However, the high-energy emission band, which is slightly blue-shifted in relation to their precursors (514 nm [Pt(bzq)(C_6F_5)$_2$]$^-$; 496 nm [Pt(bzq)(C_6Cl_5)$_2$]$^-$) reflecting the formation of the Pt → Ag dative bond, has been assigned to a ^{3}MLCT or a mixed ^{3}LC/^{3}MLCT emissive state.

The two different polymorphs of **21** show different luminescence in solid state (298 K, **21a** orange, **21b** green). The form **21b**, which packs as discrete π···π (bzq) dimers, exhibits a vibronic high-energy band (298 K: λ_{em} 510, 534 nm; 77 K: 512, 551 nm), typical of a mixed ^{3}LC/^{3}MLCT emissive state. However, the form **21a**, which possesses a long-range π···π 1D-extended structure, displays an intriguing *luminescence thermochromism* (Fig. 9). At 298 K, the emission is dominated by a broad unstructured low-energy band (orange, λ_{max} 572 nm) attributed to a ligand centered $^3\pi\pi^*$ excimeric emissive state, associated with the short intermolecular

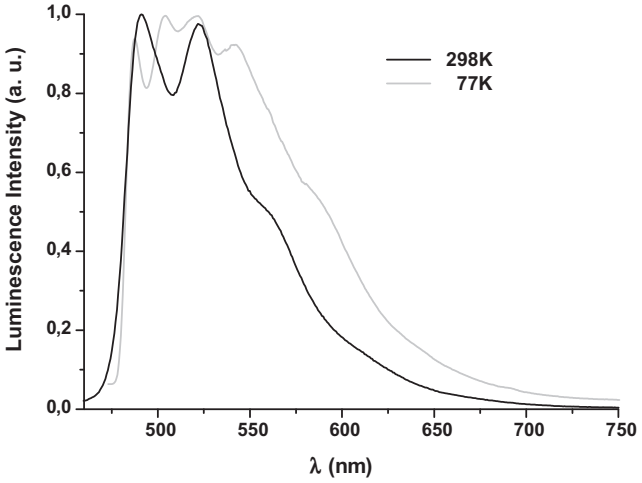

Fig. 8. Emission spectra of **22** in solid state at 298 K and 77 K (λ_{exc} 420 nm).

$\pi\cdots\pi$ interactions. At low temperature (77 K), the orange emission is not detected and the luminescence switches to a highly structured green emission (λ_{max} 512 nm) of ^{3}LC/^{3}MLCT origin. The orange emission triggered at room temperature resembles the aggregation induced emission (AIE) observed in other Pt^{II}, and more recently, Ir^{III} systems [81,106–113]. Complex **21** shows only a weak emission (506, 541 nm) in fluid CH_2Cl_2 solution, which becomes well structured at 77 K (504_{max}, 538, 585 nm) and slightly red-shifted in relation to its precursor (λ_{max} 490 nm) and to the bimetallic complexes **22** and **23** (495 nm **22**, 490 nm **23**, 77 K). This intense green emission is independent of the concentration and excitation wavelength, indicating the absence of any aggregated induced emission in frozen solution.

It is well known that Pt–M bonding interactions in cooperation with bridging ligands, usually favors the formation of multinuclear complexes. In the context of Pt^{II} cyclometalated complexes, several types of ligands have been used to keep Pt and metal (M = Cu, Ag, Au) in close proximity, thus favoring the formation of Pt–M bonds. The cyclometalated complex $[Pt_2Me_2(bzq)_2(\mu\text{-dppy})_2Ag_2(\mu\text{-acetone})](BF_4)_2$ **24** has been synthesized from the reaction of [PtMe(bzq)(dppy)], which contains one free pyridyl unit, with 1 equiv. of $[Ag(CH_3CN)_4]BF_4$ [114]. This tetranuclear cluster exhibits a central Pt_2Ag_2 core with an unprecedented butterfly skeletal geometry in which the Ag atoms occupy the edge-sharing

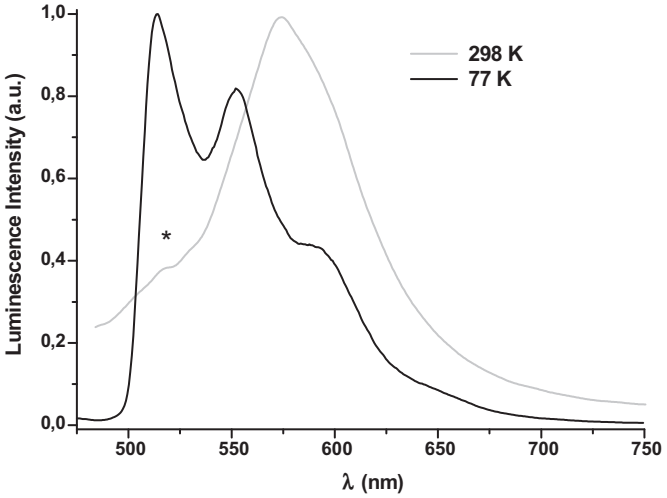

Fig. 9. Emission spectra of nearly pure **21a** (*small impurity of **21b**) in solid state at 298 K and 77 K.

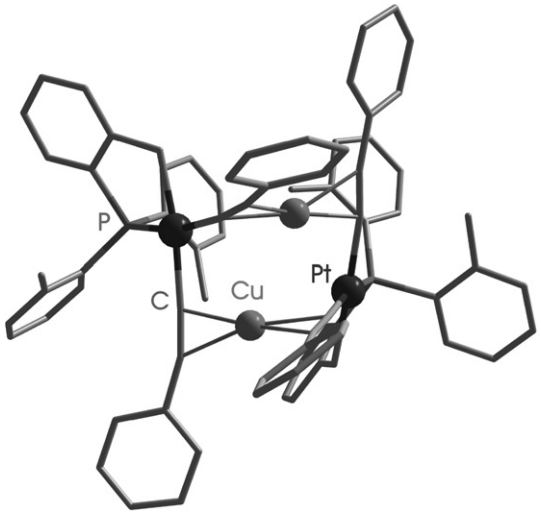

Fig. 10. Molecular structure of $[Pt\{CH_2C_6H_4P(o\text{-tolyl})_2\text{-}\kappa C,P\}(C{\equiv}CPh)_2Cu]_2$ **29**.

bond (Scheme 3). The two platinum units are linked by two Pt–Ag bonds located on the same side of the coordination plane and one metallophilic Ag–Ag bonding interaction [2.8265(5) Å], with an acetone molecule bridging the two Ag atoms [Ag–O 2.683(3) Å]. It is worth noting that despite the presence of the bridging dppy ligand [Ag–N 2.315(3) Å], the bonding of the Ag center with the Pt–C(cyclometalated) bond [Pt–Ag 2.7749(3), 3.0311(3) Å; Ag–C 2.3473(3) Å] is comparable to those seen in the previous unsupported Pt–Ag bonds in complexes **18**–**23**. The bridging acetone molecules are dissociated from the cluster **24** in solution, but the Pt_2Ag_2 core is retained as an equilibrium mixture of the butterfly and planar geometries, as is suggested by NMR data. No photoluminescence studies were reported.

The neutral dithiocarbamate cycloplatinate CˆP compound $[Pt(C\^P)(L\^L)]$ [CˆP = $CH_2C_6H_4P(o\text{-tolyl})_2$-κ*C,P*; LˆL = S_2CNMe_2] is able to act as a Lewis base towards $[M(OClO_3)(PPh_3)]$ (M = Ag, Au) or $AgClO_4$ (1:1) yielding bi-Pt–M (M = Ag **25**, Au **26**) or tetranuclear Pt_2Ag_2 (**27**) [115] derivatives (Chart 5) [116]. However, in these systems the silver center is mainly bonded to the platinum [Pt–Ag 2.875(1) Å **25**, 2.671(3) Å and 2.752(3) Å in $\mathbf{27}^+$ and $\mathbf{27}(OH_2)^+$] and to the sulfur of the dithiocarbamate group. As confirmed by X-ray diffraction studies, short metallophilic Ag···Ag [2.905(8); 2.856(3) Å] bonding interactions and the perchlorate anion contacting one of the Ag centers are also contributing to the stability of the Pt_2Ag_2 derivative **27**.

Along the same lines, Forniés et al. have shown that the bent diplatinum complexes with pyrazolate bridging ligands $[Pt_2(C\^P)_2(\mu\text{-Rpz})_2]$ (Rpz = pz, 3,5-dmpz, 4-Mepz) have an adequate arrangement to act as a chelating ligand of a silver center. The precursors react with $AgClO_4$ (1:1) to give the trinuclear compounds Pt_2Ag **28** (Chart 5), in which the Ag^I forms two Pt–Ag bonds [R = 4-Mepz, Pt–Ag: 2.783(1), 2.788(1) Å] and completes its electronic requirements with two η^2-aryl bonding interactions from the *o*-Tol groups [117].

With the same cyclometalated CˆP ligand, the monoanionic bis(alkynyl)platinum(II) complex $(NBu_4)[Pt(C\^P)(C{\equiv}CPh)_2]$ reacts with M^I (M = Cu, Ag) affording discrete tetranuclear clusters $[Pt(C\^P)(C{\equiv}CPh)_2M]_2$ (M = Cu **29**, Ag **30**) [118]. The crystal structure of **29** shows that both "$Pt(C\^P)(C{\equiv}CPh)_2$" fragments (dihedral angle ~124°) are connected by two Cu^I centers through η^2-alkynyl bonds, in agreement with the stronger preference of the M^I (Cu, Ag) for the electron-rich alkynyl units than for the basic Pt^{II} center (Fig. 10) [55]. No photophysical properties of these CˆP complexes were reported.

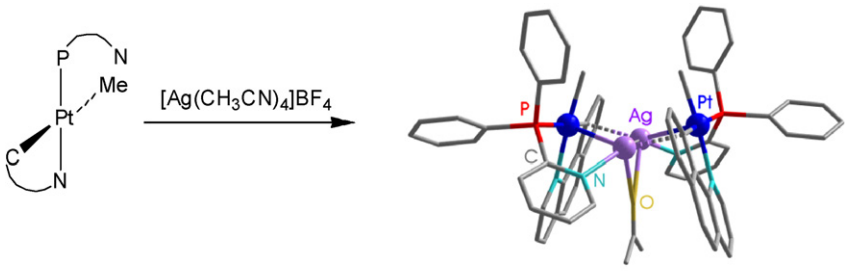

24

Scheme 3.

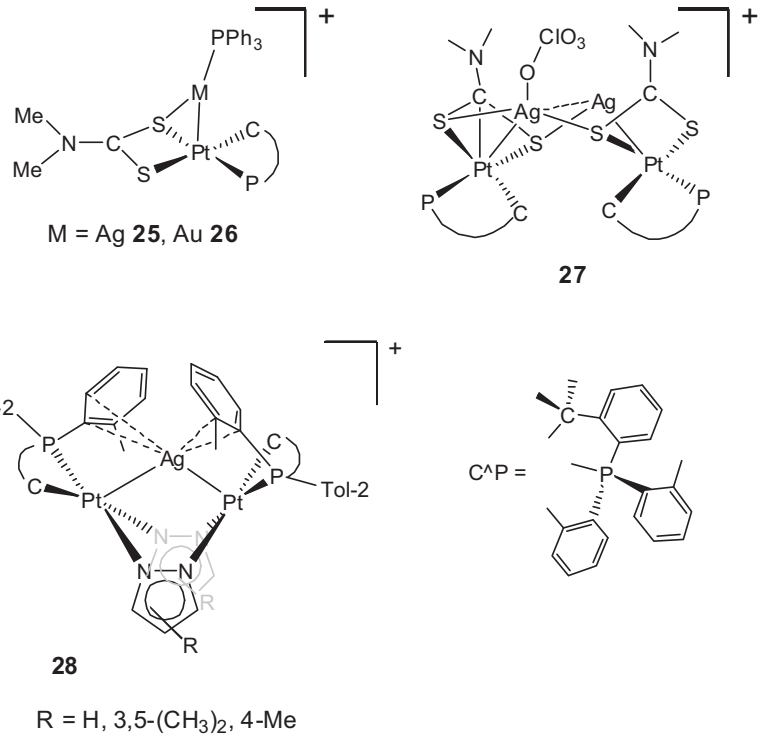

Chart 5.

Heteropolynuclear systems based on monoalkynyl cycloplatinate fragments are scarce. Reactions of the cyclometalated complex {Pt}(C≡CSiMe$_3$) ({Pt} = [Pt(C$_6$H$_3${Me$_2$NCH$_2$}$_2$-2,6)]$^+$) with [Cu(NCMe)$_4$]$^+$ or Ag$^+$ also afford heterotrinuclear cationic complexes **31** in which both alkynyl units are η^2 coordinated to a M^I center (Chart 6) [79]. However, the attachment of the functionalized {Pt}(C≡C–C$_6$H$_4$CN-4) to AuCl (**32**, Chart 6), occurs via the η^1-coordination of the–C≡N function [79]. Related to this, Me$_3$SiC≡C{Pt}Cl forms the linear heterometallic complex PPh$_3$AuC≡C{Pt}Cl **33** by reaction with AuCl(PPh$_3$)/NEt$_2$H, CuCl (*cat*), which further reacts with Me$_3$SnC≡CFc to yield PPh$_3$AuC≡C{Pt}C≡CFc **34** (Chart 6) [78]. Electrochemical studies revealed that the reversible oxidation of the Fc units in Me$_3$SiC≡C{Pt}C≡CFc and **34** and the irreversible Pt^{II}/Pt^{IV} oxidation are both facilitated supporting electronic communication through the conjugated Pt–C≡C-unit.

An unexpected Pt$_2$Cu$_6$ heteropolynuclear alkynyl cluster [Pt$_2$Cu$_6$(bzq)$_2$(C≡C–C$_5$H$_4$N-2)$_6$I$_2$] **35** is generated by reaction of [Pt(bzq)(μ-Cl)]$_2$ with 2-ethynylpyridine (HC≡C–C$_5$H$_4$N-2) and CuI in the presence of NEt$_3$ [119]. The molecular structure of **35** consists of a central hexanuclear dicationic copper core [Cu$_6$(C≡C–C$_5$H$_4$N-2)$_2$I$_2$]$^{2+}$ assembled by two monoanionic

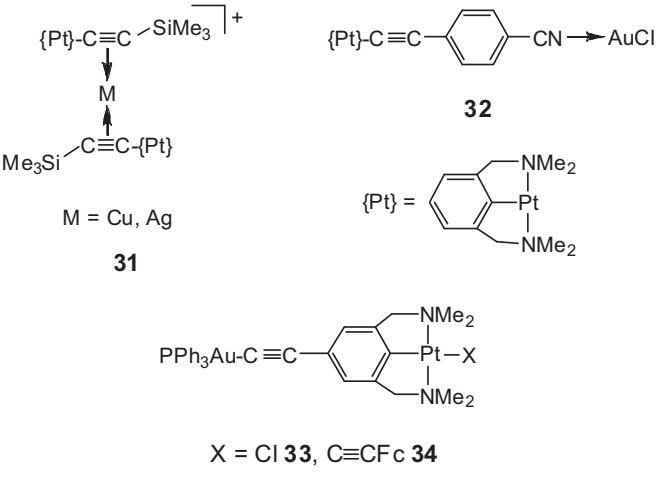

Chart 6.

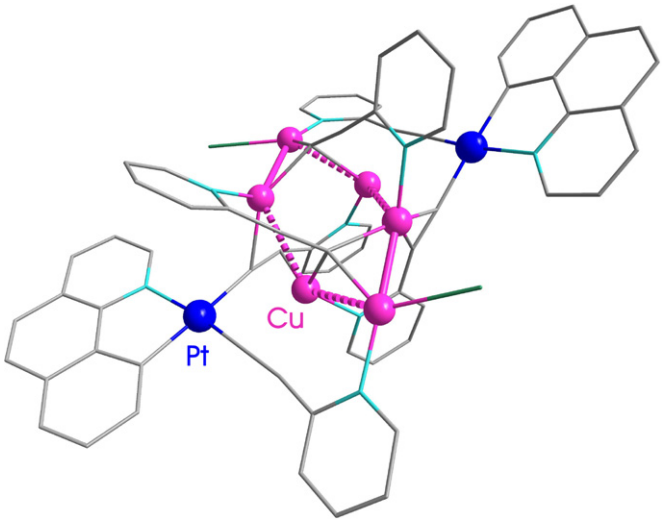

Fig. 11. Schematic view of $[Pt_2Cu_6(bzq)_2(C{\equiv}C\text{-}C_5H_4N\text{-}2)_6I_2]$ **35**.

benzoquinolate-dialkynylplatinate(II) $[Pt(bzq)(C{\equiv}C\text{–}C_5H_4N\text{-}2)_2]^-$ fragments (Fig. 11). The central copper core forms a distorted six-membered boat (open book shape) with two very short [2.5185(11), 2.5338(10) Å] and four longer [2.8189(11)–3.0327(11) Å] Cu···Cu interactions and, as result, three different copper environments and alkynyl coordination modes are found (μ-κC^{α}:κN; μ_3-κC^{α}:η^2:κN and the rare μ_4-κC^{α}:κN bridging mode) in the cluster. In solid state at 298 K, the cluster shows an orange emission (638 nm, 10.9 μs), which is slightly red-shifted to 660 nm (18.9 μs) at 77 K. However, in fluid CH_2Cl_2 solution, the cluster **35** exhibits two broad emissions (560 nm, 635 nm), which are better resolved and slightly blue-shifted at 77 K (540 nm, τ = 70 μs; 615 nm, τ = 59 μs), suggesting the existence of two close excited states. Although the assignment of the luminescence of the cluster is not straightforward, it has been suggested that the low-energy emission observed in solid state and in CH_2Cl_2 (298, 77 K) could derive from an excited state involving the short Cu···Cu interactions, with a ^{3}LMCT [2-pyridylethynyl → Cu_n] origin, probably combined with a Cu^I centered d/sp character. The high-energy emission seen in CH_2Cl_2 at 298 K and in glass state (77 K) could be originated from intraligand $^3\pi\pi^*$ (2-pyridylethynyl) excited states, associated with the Pt fragments perturbed by coordination to Cu^I.

Following this first report on the platinum-copper alkynyl benzoquinolate cluster **35**, our research group has been involved in carrying out detailed investigations on a series of Pt^{II}–Cu^I cyclometalated (bzq, ppy) systems with different alkynyl ligands (C≡CR, R = ^{t}Bu, Ph, $C_6H_4OCH_3$-4, $C_6H_4OCH_3$-3, $C_6H_4OCF_3$-4, $C_6H_4C{\equiv}CPh$). We have found that related reaction systems ($[Pt(bzq)(\mu\text{-}Cl)]_2$/HC≡CR, CuI, base) are a successful route to the synthesis of tetranuclear brightly emissive clusters $[Pt_2Cu_2(C^{\wedge}N)_2(C{\equiv}CR)_4]$ **36** (Chart 7) [120,121]. X-ray diffraction studies reveal a sandwich type structure in which two anionic platinate fragments $[Pt(C^{\wedge}N)(C{\equiv}CR)_2]^-$ are connected by two centers through strong η^2-alkynyl Cu^I bonds and weaker metallophilic Pt···Cu and Pt^{II}···Pt^{II} contacts. The neutral nature of the clusters and the planarity of the aromatic cyclometalating ligands facilitate the occurrence of polymorphism (R = $C_6H_4C{\equiv}CPh$) or the formation of extended stacking (Pt···Pt/π···π) networks (R = C_6H_4OMe-3) with interesting solid-state emissions, including vapochromism. Continuing research in this area, we have extended this chemistry to silver and we have also prepared related Pt_2Ag_2 clusters using different synthetic routes, in order to establish their structure-property relationship. Details of these complexes will be reported elsewhere.

3. Heteronuclear platinum-group 12 metal complexes

Although several cycloplatinated heteropolymetallic systems involving simple $Pt^{II} \rightarrow Hg^{II}$ donor–acceptor or covalent Pt–Hg have been reported (Chart 8), no emissive properties have been described.

The metal C^P cyclometalated complexes $[Pt(C^{\wedge}P)(S_2C\text{-}Z)]$ [C^P = CH_2-C_6H_4-P(*o*-tolyl)$_2$-$\kappa C,P$; Z = NMe_2, OEt] react with HgX_2 to form tetranuclear compounds **37**, in which the platinum fragments are acting as donors to mercury only through the Pt atom [Pt → Hg = 2.768(1) Å] [122]. By contrast, the analogous reaction of $[Pt(C^{\wedge}P)(S_2C\text{-}NMe_2)]$ with $Hg(O_2CR)_2$ (1:1 molar ratio) takes place through a stereoselective *cis* oxidative addition, affording the binuclear complexes **38**, containing a short unsupported Pt → Hg covalent bond, as confirmed by X-ray [R = CF_3; Pt–Hg = 2.5535(7) Å] [123].

Along the same lines, complex $[Pt(C^{\wedge}P)(acac\text{-}O,O')]$ with HgX_2 (X = I, Br) (1:1) gives the tetranuclear $[Pt(C^{\wedge}P)(acac\text{-}O,O')HgI(\mu\text{-}I)]_2$ **39** and pentanuclear $[\{Pt(C^{\wedge}P)(acac\text{-}O,O')HgBr(\mu\text{-}Br)\}_2(\mu\text{-}HgBr_2)]$ **40** complexes, containing unsupported donor–acceptor Pt → Hg bonds. However, its reaction with $Hg(O_2CR)_2$ (1:2 molar ratio) evolves with substitution of the acac ligand, affording hexanuclear complexes $[Pt(C^{\wedge}P)(\mu\text{-}O_2CR)_2Hg(\mu_3\text{-}acac\text{-}\kappa C^3,O)Hg(O_2CR\text{-}\kappa O)]_2$ (R = CH_3, CF_3) **41**, having very short Pt → Hg donor bonds supported by two carboxylate groups, along with an unusual

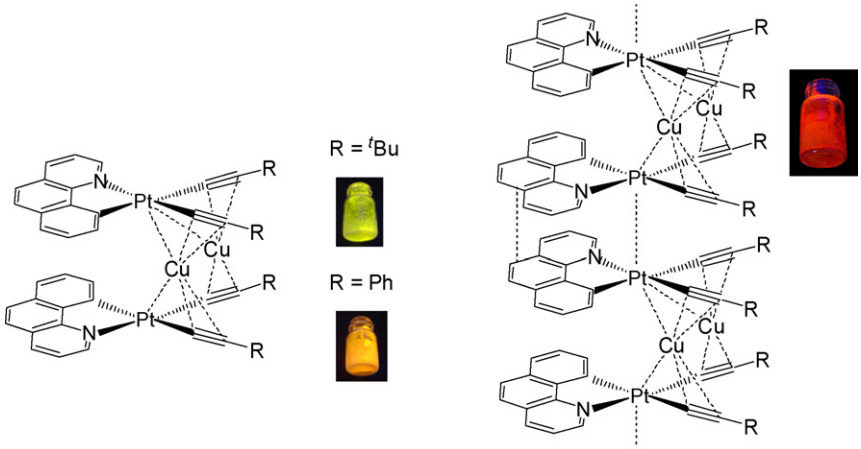

36

Chart 7.

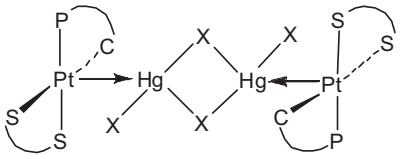

S S = S_2CNMe_2, S_2COEt
X = Br, I

37

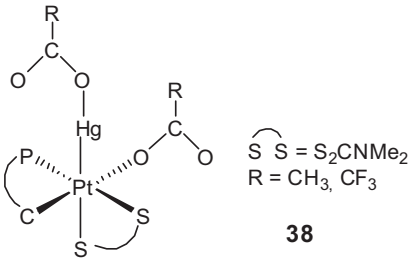

S S = S_2CNMe_2
R = CH_3, CF_3

38

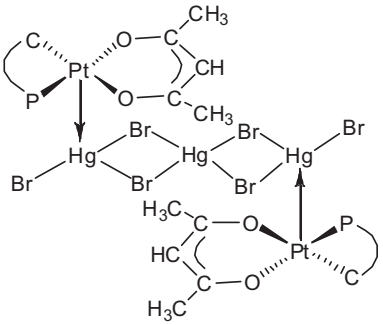

40

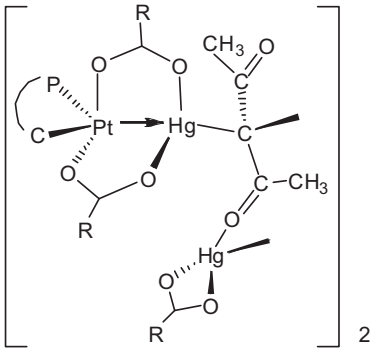

R = CH_3, CF_3

41

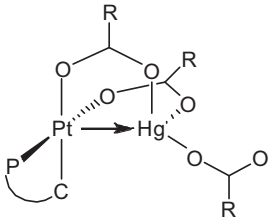

R = CH_3, CF_3

42

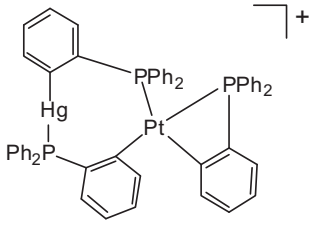

44

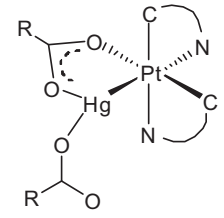

C N = 2-$Me_2NCH_2C_6H_4$, $2Me_2NC_6H_4CH_2$
R = CH_3, iPr

45

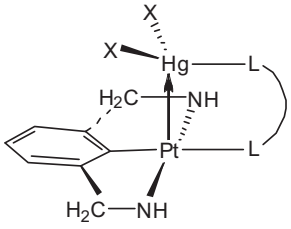

L L = O_2CR; R = Me, i-Pr; X = Br, O_2CR; R = i-Pr; X = Cl

L L = NYNR; Y = CH, N; R = Me, Et, i-Pr
X = Br, Cl

46

Chart 8.

dimercuriated acetylacetonate units [R = CH_3, Pt–Hg 2.6498(9) Å] [124]. Robust bimetallic double bridged carboxylate derivatives **42** [125] (Chart 8) are also generated by treatment of [{Pt(C^P)(μ-O_2CR)}$_2$] with 2 equiv. of HgX_2 (X = O_2CR, R = CH_3, CF_3; halide). The molecular structure of **42** (R = CH_3) confirms the presence of a strong Pt → Hg donor bond [2.6131(6) Å], comparable to those found in systems with covalent bonds; which are also in agreement with the values of $^2J^{199}$Hg-^{31}P (98–161 Hz) observed in solution.

Aryl transfer from [Hg(2-$C_6H_4PPh_2$)$_2$] to [$PtCl_2$(COD)] gives the cyclometalated $Pt^{II} \rightarrow Hg^{II}$ [3.1335 Å] complex [Pt(C^P)(μ-2-$C_6H_4PPh_2$)$_2$HgCl] **43** (C^P = 2-diphenylphosphinophenyl) from which the salt **44** (Chart 8) is obtained by treatment with $AgPF_6$ [126].

The electron rich bis(cyclometalated) complexes *cis*-[Pt(C^N)$_2$] (C^N = 2-$Me_2NCH_2C_6H_4$; 2-$Me_2NC_6H_4CH_2$) react with Hg(O_2CR)$_2$ (R = Me, iPr) to yield, after *cis*-oxidative addition, *cis,cis*-[(C^N)$_2$(μ-O_2CR)PtHg(O_2CR)] [127] **45,** having a bridging acetate group

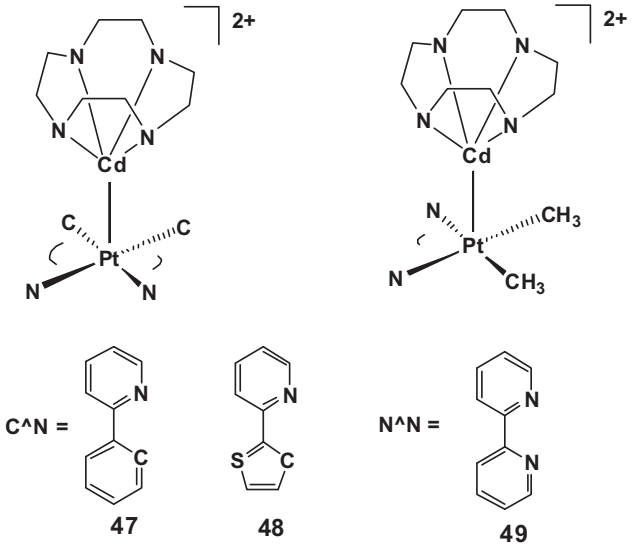

Chart 9.

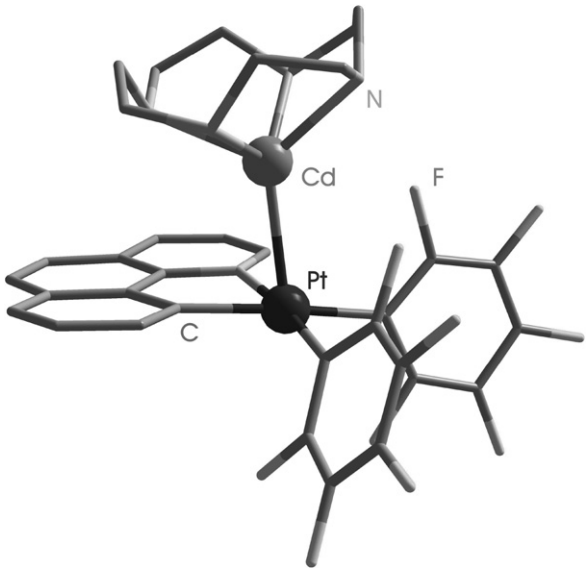

Fig. 12. Structure of the cation $[(C_6F_5)_2(bzq)PtCd(cyclen)]^+$ in complex **50**.

supporting the covalent Pt–Hg bond [2.513(1) Å] as confirmed by X-ray on $[(2\text{-}Me_2NCH_2C_6H_4)_2(\mu\text{-}MeCO_2)PtHg(O_2CMe)]$. Curiously, similar reactions of mercury(II) salts such as $Hg(O_2CR)_2$ (R = Me, iPr) [127] and [Hg{(*p*-tol)NYNR}Cl] (Y = CH, N; R = Me, Et, i-Pr) [128] with the terdentate (NˆCˆN) complexes [{2,6-$(Me_2NCH_2)_2C_6H_3$}PtX] resulted in the formation of complexes **46,** having a five-coordinate Pt center and one bidentate anionic (carboxylate, formamidinate or triazenido) bridging a $Pt^{II} \rightarrow Hg^{II}$ donor bond, as confirmed by X-ray on [{2,6-$Me_2NCH_2)_2C_6H_3$}Pt(μ-{(*p*-tol)NC(H)N(i-Pr)}HgBrCl] [128].

As commented before, the strong ligand field caused by cyclometalated ligands favors the formation of strong dative $Pt^{II} \rightarrow M$ bonds. In fact, the first examples of platinum(II)–cadmium(II) bonds were described by Ito and coworkers [129] in complexes **47**–**49** easily formed by reacting *cis*-[Pt(ppy)$_2$], *cis*-[Pt(thpy)$_2$] and also *cis*-[Pt(CH$_3$)$_2$(bpy)] with [Cd(cyclen)(MeOH)$_2$](ClO$_4$)$_2$ in a 1:1 molar ratio. The Pt–Cd distances found in the cations $\mathbf{47^{2+}}$ [Pt–Cd 2.639(1) Å] and $\mathbf{49^{2+}}$ [Pt–Cd 2.610(1) Å] (Chart 9) are remarkably shorter than the sum of the metallic bond radii (2.88 Å), indicating the formation of strong unsupported $Pt^{II} \rightarrow Cd^{II}$ bonds. Although remarkable hypsochromic color shifts were observed in the formation of **47**–**49**, no distinct absorption appeared in their electronic spectra in solution and partial dissociation was suggested on the basis of ^{195}Pt NMR spectroscopy. No emission studies were reported.

Following a similar synthetic strategy, Forniés, Lalinde et al. reported the less charged cationic complex $[(C_6F_5)_2(bzq)PtCd(cyclen)](ClO_4)$ **50** (Fig. 12) using $(NBu_4)[Pt(bzq)(C_6F_5)_2]$ as precursor [130]. As in **47** and **49**, the Cd^{2+} ion is in a square pyramidal coordination geometry with the four N of the cyclen forming the basal plane and the donor Pt atom at the apex. Despite the presence of the bulky C_6F_5 groups, the Pt–Cd bond distance in $\mathbf{50^+}$ [2.688(1) Å] is comparable to that seen in $\mathbf{47^{2+}}$ [2.639(1) Å]. As can be seen in Fig. 12, the Cd moves away from the C_6F_5 groups with the Pt–Cd bond tilted by 17.6(2)° (13.0° for **47** and 6.8° for **49**) from the platinum plane, indicating the absence of *ortho*-fluorine···Cd contacts.

The formation of the Pt–Cd bond in **50** is clearly inferred from the comparison of its photophysical properties with those of the starting precursor $(NBu_4)[Pt(C_6F_5)_2(bzq)]$. In CH_2Cl_2, complex **50** shows a low-energy absorption band, blue-shifted (410 nm) with respect to that observed in the precursor (425 nm), in agreement with the presence of the Pt–Cd bond, which produces an increase in the electrophilicity of the Pt center, resulting in a blue-shift for this ^{1}MLCT absorption. Complex **50** displays in the solid state a more structured (298 K, λ_{max} 490 nm; 77 K, λ_{max} 484 nm) and slightly blue-shifted emission in relation to that of the mixed ^{3}IL/^{3}MLCT manifold of the precursor [298 K, λ_{max} 518 nm (broad); 77 K, λ_{max} 514 nm (structured)] (Fig. 13). The shift is consistent with the influence of a dative Pt → Cd bond, which likely stabilizes the HOMO increasing the corresponding HOMO–LUMO gap. It is also in agreement with some degree of charge transfer (^{3}MLCT) for the transition, since the Cd^{2+} ion drains electron density from the Pt, making the transfer of charge away from the metal a more energetic process. A similar hypsochromic shift is also seen in fluid and frozen acetone. It is worth to note that the formation of the Pt → Cd bond causes a significant decrease in the lifetime of the solid emission at 298 K (7.9 μs **50** *vs.* 16.5 μs precursor) and an increase in the luminescence efficiency in solution [Φ 0.0285 ($K_r = 3.6 \times 10^3\ s^{-1}$) **50** *vs.* 0.0019 ($K_r = 0.115 \times 10^3\ s^{-1}$) precursor].

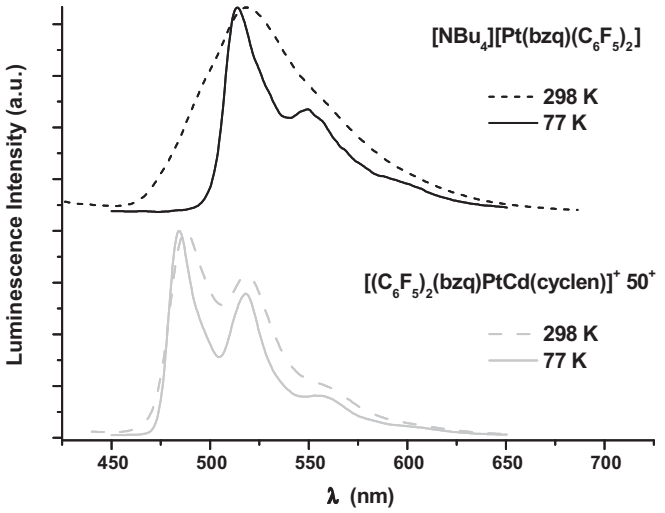

Fig. 13. Emission spectra of $[(C_6F_5)_2(bzq)PtCd(cyclen)](ClO_4)$ **50** and of its precursor $(NBu_4)[Pt(bzq)(C_6F_5)_2]$ in solid state at 298 K and at 77 K.

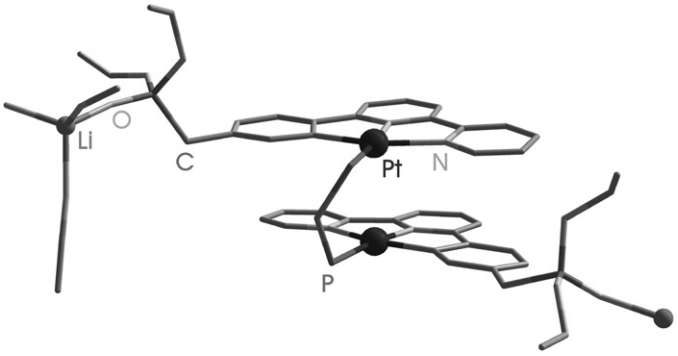

Fig. 14. View of part of the chain formed in the cationic unit $[Pt_2(N^{\wedge}N^{\wedge}CPO)_2(\mu\text{-dppm})Li(CH_3CN)_2]^{3+}$ in **51**.

4. Heteronuclear platinum-main group metal complexes

A one-dimensional "staircase" Pt^{II}–Pt^{II}–Li^{I} coordination polymer $[\{Pt_2(N^{\wedge}N^{\wedge}CPO)_2(\mu\text{-dppm})Li(CH_3CN)_2\}\{ClO_4\}_3]_n$ **51** [N^N^CHPO = 6-[4-(diethoxyphosphorylmethyl)phenyl]-2,2′-bipyridinyl] has been synthesized by treatment of [Pt(N^N^CPO)Cl] with dppm and excess of $LiClO_4$ [131]. In this chain, diplatinum μ-dppm dicationic "$Pt_2(N^{\wedge}N^{\wedge}CPO)_2(\mu\text{-dppm})$" units with a close Pt···Pt distance of 3.1423(9) Å are linked through the oxygen atoms of the phosphonate group of neighboring ligands, both coordinated to a $Li(NCMe)_2$ moiety (Fig. 14). Coordination of the external hinged phosphoryl groups to the Li^+ centers only causes minor structural and electronic modifications in relation to the diplatinum monomer complex $[Pt_2(N^{\wedge}N^{\wedge}CPO)_2(\mu\text{-dppm})](ClO_4)_2$, $[Pt_2](ClO_4)_2$, which also exhibits a close Pt···Pt separation of 3.325(2) Å. Thus, both complexes displayed two absorption bands at λ_{max} 420 and 480(sh) nm, which were assigned to metal–metal-to-ligand charge transfer on the basis of DFT calculations performed on the monomer $[Pt_2]^{2+}$. The luminescent behavior both in solution [645 nm, τ = 0.36 μs, Φ = 0.022 in **51** *vs.* λ_{max} 649 nm, τ = 0.34 μs, Φ = 0.021 in $[Pt_2](ClO_4)_2$] and in solid state [635 nm **51** *vs.* 630 nm in $[Pt_2](ClO_4)_2$] is also similar. The HOMO and LUMO characteristics have suggested an assignment of the excited state in both complexes as ^{3}MMLCT [$d\sigma^*(Pt_2) \rightarrow \pi^*$] with the HOMO coming from the Pt···Pt interaction and the LUMO mainly located on the conjugated aromatic ligand.

Recently, the nitrile cationic complexes $[Pt(C^{\wedge}N)(NCMe)_2]ClO_4$ [C^N = bzq and ppy] have been used by Forniés et al. as precursors for the preparation of anionic cyanide derivatives $[Pt(C^{\wedge}N)(CN)_2]^-$, which have been isolated not only with $(NBu_4)^+$ but also as the potassium $[K(H_2O)][Pt(C^{\wedge}N)(CN)_2]$ **52A**, **53A** salts [132]. In these species, the cation plays an important role, not only on their solubility but also on their optical properties, the potassium salts (**52A** and **53A**) being water-soluble and strongly colored (red **52A** or purple **53A**). Interestingly, they transform in a reversibly fashion into the yellow compounds $K[Pt(C^{\wedge}N)(CN)_2]$ (C^N = bzq **52B**, ppy **53B**) upon slow desorption and fast reabsorption of the water molecules of the environment (Scheme 4).

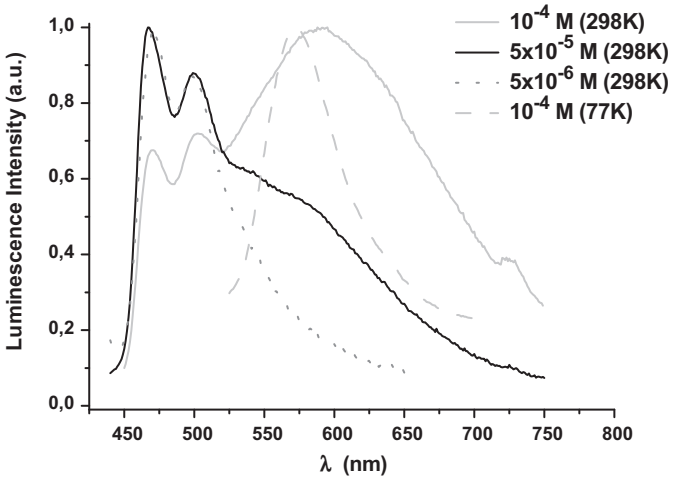

Fig. 16. Emission spectra of $[K(H_2O)][Pt(bzq)(CN)_2]$ **52A** in water.

Crystallization of **53B** from acetone provided crystals of stoichiometry $[K(OCMe_2)_2][Pt(ppy)(CN)_2]$ **53C**, that formed an interesting extended network involving the two CN^- ligands as bridging between Pt and different potassium ions of the countercation $[\{K(OCMe_2)(\mu\text{-}OCMe\}_2]^+$ (Fig. 15).

In methanol solution, the potassium compounds exhibit, as expected, identical photophysical properties to those of monomers $(NBu_4)[Pt(C^{\wedge}N)(CN)_2]$, assigned to mixed ^{3}LC/^{3}MLCT transitions on the basis of TD-DFT calculations. However, **52** and **53** are also soluble and luminescent in H_2O (298, 77 K) (Fig. 16), showing typical ^{3}LC/^{3}MLCT emission at low concentration and additional excimeric $^3\pi\pi^*$ features at higher concentration and/or in frozen glasses. In addition, these potassium salts show intriguing solid-state properties. The hydrated colored solids **52A** and **53A** show a characteristic

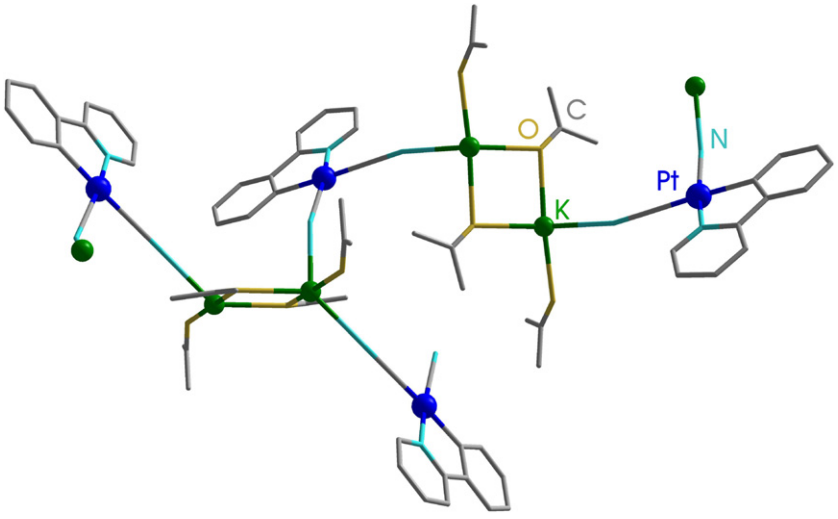

Fig. 15. Molecular structure of $[K(OCMe_2)_2][Pt(ppy)(CN)_2]$ **53C**.

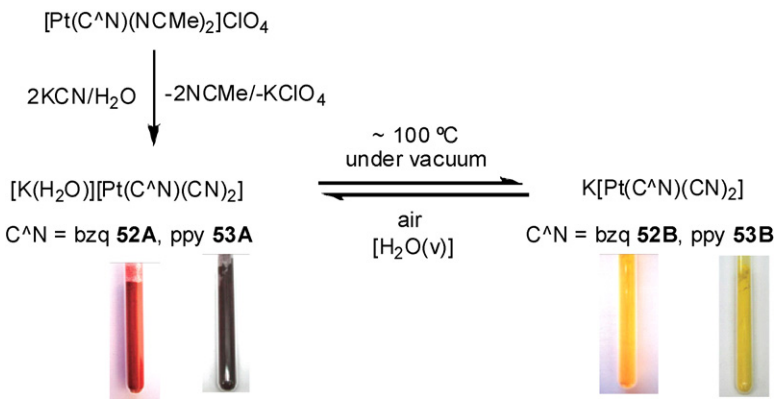

Scheme 4.

low energy absorption (548 nm **52A**; 564 nm **53A**), as well as a structureless emission ($\lambda > 700$ nm) (Fig. 17) red-shifted upon cooling to 77 K (~40 nm), that the authors attributed to typical MMLCT [$d\sigma^*(Pt) \rightarrow \pi^*(C\hat{}N)$] transitions, associated with the occurrence of short Pt···Pt contacts in these forms. In the unsolvated yellow solids (**52B** and **53B**), the emission, however, is not dependent on the temperature and appears remarkably blue-shifted (structureless band 636 nm) with respect to the hydrated forms in the typical region of the $\pi\cdots\pi$ stacked Pt^{II} complexes. In these yellow unsolvated solids, the emission seems to be dominated by $\pi\cdots\pi$ interactions although the presence of short Pt···Pt contacts in the solids has not been ruled out.

It is worth to note that the hydrated **52A** also exhibits a reversible vapochromic behavior by changing its color from red to yellow upon exposure to some volatile organic compounds (VOCs) such as CH_2Cl_2, MeOH, EtOH, acetone, THF (Fig. 18), the shortest response times shown for methanol (5 s) and ethanol (10 s). The vapochromic response cycle was repeated with no noticeable chemical decomposition of **52A**. However, the purple phenylpyridinate derivatives **53A** does not show vapochromic behavior, a feature likely due to stronger bonding of the H_2O molecules in the lattice.

Another water-soluble K^+/Pt^{II} complex [K(18-crown-6)][Pt(ppy)Cl_2]·0.5H_2O **54** has been prepared from [18-crown-6]$_2$[$PtCl_4$] and 2-phenylpyridine with the goal of examining the photochemical H_2 production in aqueous media [133]. Two independent sets of ion pairs with the rare Pt(μ-Cl)$_2$K core were found in the asymmetric unit, one with an aqua ligand coordinated to the potassium atom [K(18-crown-6)(OH_2)][Pt(ppy)Cl_2] **54A** and the other no aqua ligand [K(18-crown-6)][Pt(ppy)Cl_2] **54B** (Fig. 19). Slow hydrolysis was observed in solution, which has been examined by UV–vis absorption spectroscopy and TD-DFT calculations.

A rare cycloplatinate adduct of the "*in situ*" generated amide complex K[Pt(pap)(O^{t}Bu)] [H_2pap, 2-phenyl-6-(2-aminoisopropyl)pyridine;] has been isolated as [{Pt(pap)}$_2$(KCl){KO^{t}Bu}$_8$] **55** [134]. As shown by single X-ray diffraction, **55** contains two Pt(pap) moieties, which are attached to a central metal–oxygen network templated by a Cl^- of stoichiometry K_9O_8Cl, through Pt–O, N(amido)-K^+ bonds and $\pi\cdots K^+\cdots$aryl (pap) interactions.

As is frequently observed with related cationic platinum polypyridine complexes, which have been examined as effective sensors by incorporating functionalized acetylide groups as ion host units [46,48,135–141], several neutral cycloplatinated systems have been reported. Wu, Tung et al. [142] attached an azacrownether group to the alkynyl coligand of the cycloplatinated C^N^N complex (**56**) and investigated its ion binding properties (Chart 10). Although significant color changes were observed upon addition of Li^+, Na^+, K^+, Ba^{2+}, Ca^{2+} or Mg^{2+} to **56**, only Mg^{2+} produced a remarkable increase in the luminescence intensity.

The electronic spectrum of **56** displayed a low energy band at ~500 nm, which was assigned as ligand-to-ligand charge transfer (^{1}LLCT) (alkynyl $\rightarrow$ C^N^N) transition, and a band at 390–470 nm, ascribed to the ^{1}MLCT (Pt $\rightarrow$ C^N^N). Upon complexation of alkali or alkaline earth metal ions (Li^+, Na^+, K^+, Ba^{2+}, Ca^{2+} or Mg^{2+} as ClO_4^- salts), the ^{1}LLCT transition band disappeared and an increase of intensity of the metal-to-ligand charge transfer ^{1}MLCT was observed with a well-defined isosbestic point (465 nm for Mg^{2+}) (Fig. 20a). This behavior is consistent with the fact that complexation of the ions to the azacrown moiety decreases its electron-donating ability, shifting the ^{1}LLCT to higher energy, and,

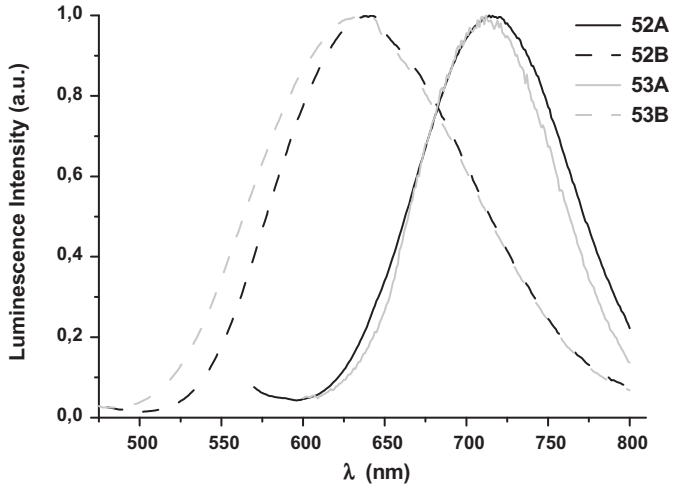

Fig. 17. Emission spectra of [K(H_2O)][Pt(C^N)(CN)$_2$] (C^N = bzq **52A**, ppy **53A**) and K[Pt(C^N)(CN)$_2$] (C^N = bzq **52B**, ppy **53B**) in solid state at 298 K.

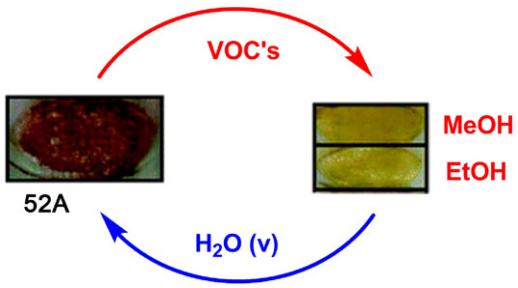

Fig. 18. Vapochromic behavior of **52A**.

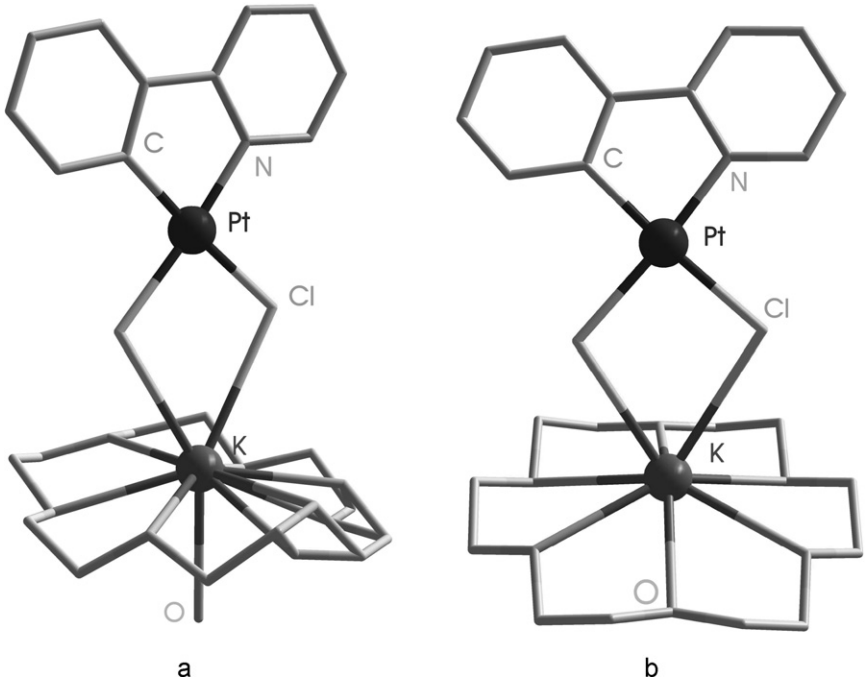

Fig. 19. Structures of [K(18-crown-6)(OH_2)][Pt(ppy)Cl_2] (**54A**) and [K(18-crown-6)][Pt(ppy)Cl_2] (**54B**).

as a consequence, the ^{1}MLCT becomes the lowest energy absorption. Complex **56** is non-emissive being attributed to rapid internal conversion from the ^{3}MLCT to the ^{3}LLCT and facile non-radiative deactivation of the low energy ^{3}LLCT state. Upon addition to Mg^{2+}, the complexed form (**56**···**Mg^{2+}**) exhibited bright luminescence from its ^{3}MLCT state at 570 nm (Φ = 0.023, τ = 180 ns) (Fig. 20b). **56** did not show any emission upon binding Li^+, Na^+, K^+, Ca^{2+} and Ba^{2+} (ions with lower charge density), which was attributed by the authors to the occurrence of facile ion dissociation caused by the excited Pt^{III} center, being more electrophilic than Pt^{II} in the ground-state. Stoichiometry (1:1) and bonding constants were similar to those of other metal-based aza-15-crown-5-ionophores [139,141]. Interestingly, complex **56** was found to signal Mg^{2+} specifically, even in the presence of high concentrations of the other commented ions.

Following a similar strategy, Guerchais, Fillaut, Williams and coworkers have prepared luminescent cycloplatinated complexes featuring an acetylide-linked flavone moiety incorporating various

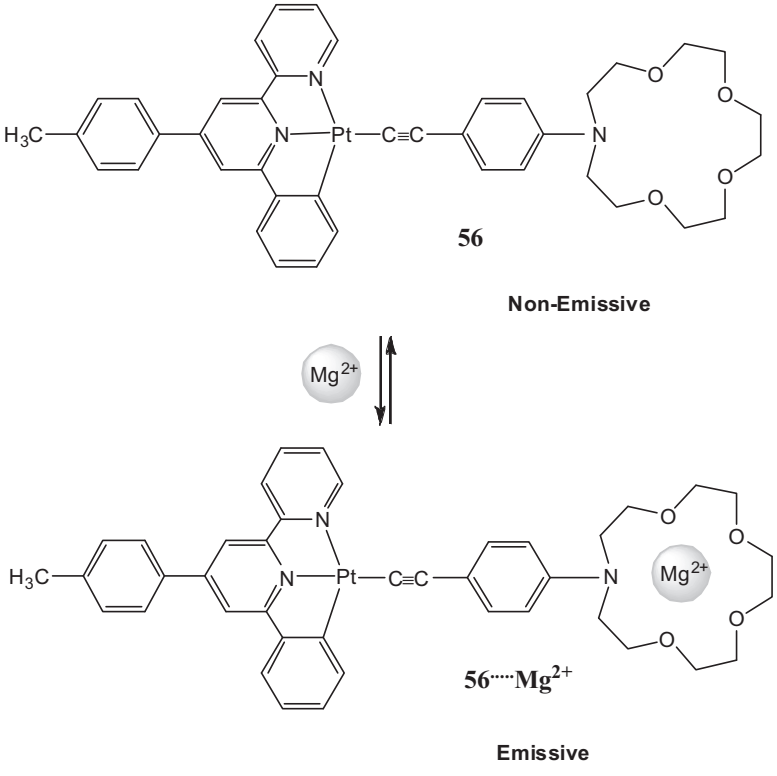

Chart 10.

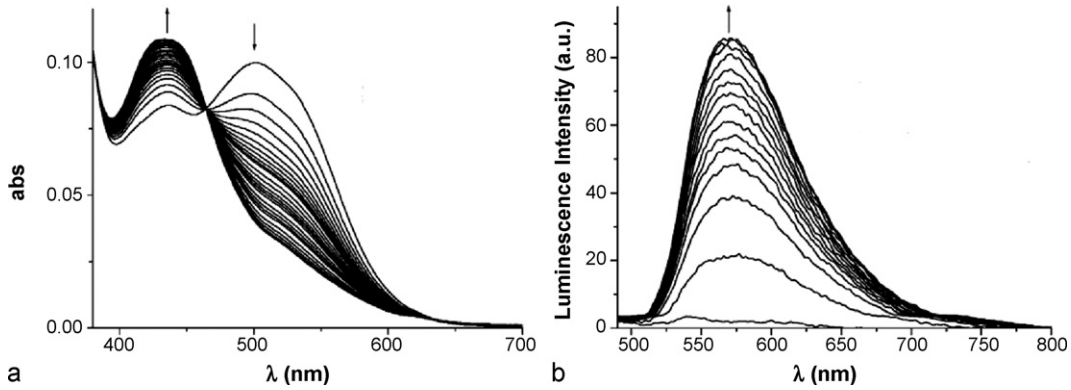

Fig. 20. (a) Changes in absorption spectrum of **56** in acetonitrile 1.2×10^{-5} M upon addition of Mg^{2+} and (b) emission spectra of **56** in acetonitrile 1.2×10^{-5} M in the presence of Mg^{2+}.
Reprinted with permission from Ref. [142]. Copyright 2010. American Chemical Society.

polyether arms (**57a–c**, Chart 11) and their binding ion (Mg^{2+}, Ca^{2+}, Cd^{2+}, Ni^{2+}, Zn^{2+}, Pb^{2+}) response was examined. Interestingly, complex **57b** produces a remarkable and selective spectral response to Pb^{2+} ion, allowing optical detection [143]. Whereas **57c** also interacts with Cd^{2+} and Ca^{2+}, no response was observed for **57a**, thus suggesting that the cation affinities can be modified through the modification of the polyether arm.

The absorption spectra of **57b**···**Pb** with increasing amounts of Pb^{2+} show a remarkable decrease in the peak intensity attributed to the IL band (~360 nm) (hypochromicity with a blue-shift) and an increase in the intensity of the low-energy [$d\pi(Pt) \rightarrow \pi^*$(phbpy)] MLCT transition located at ~420 nm. More remarkable was the influence on the photoluminescence of **57b**, which displayed a clear switch to flavone localized ^{1}IL fluorescence upon addition of Pb^{2+} (**57b**···**Pb**). In deareated acetonitrile solution, the platinum monomer exhibits a long-lived unstructured emission mainly attributed to platinum perturbed ^{3}IL phosphorescence (567 nm, $\tau \sim 20$ μs) associated with the remote flavonol unit. Upon addition of Pb^{2+}, this emission band decreased and a new structured band at ~450 nm ($\tau = 1.7 \pm 0.5$ ns) was triggered, assigned by the authors to flavonol-based fluorescence. The temporal decay on the tail of the fluorescence, in deareated solution, in the presence of excess of Pb^{2+} indicates the presence of an additional weak second component (~570 nm) of lifetime ~700 ns, which has been assigned to the emission coming from a typical ^{3}MLCT state associated with the "Pt(CˆNˆN)(C≡C)" unit. These changes upon Pb^{2+} binding have been rationalized on the basis of the occurrence of a partial decoupling of flavone orbitals (^{1}IL flavone) from those of the "Pt(CˆNˆN)(C≡C)" unit, leading to dual emission (^{1}IL from the flavone and ^{3}MLCT). Interestingly, in aerated solution, complex **57b** is not emissive due to efficient quench of the initial phosphorescence. As a consequence under these conditions, the effect of Pb^{2+} is to "*switch on*" the fluorescence of the flavonol. The complexation of Pb^{2+} in **57b**···**Pb** (1:1) is believed to occur via the formation of a chelate involving the oxygen atoms of the C=O group and terminal oxygen of the polyether arm.

In order to provide increased metal cation affinity and higher selectivity, a new cycloplatinated complex (**58**) incorporating a pyridyl unit within a macrocycle σ-alkynyl ligand has been recently designed (Scheme 5) and its ion-binding properties towards various metal cations (Ba^{2+}, Mg^{2+}, Ni^{2+}, Zn^{2+}, Pb^{2+} and Cd^{2+}) have also been explored [144].

Complex **58** exhibited only a specific response towards Pb^{2+}, which was associated with a change in the nature of the excited charge transfer state, resulting in the appearance of a low-energy absorption band and a partial quenching of its luminescence. This

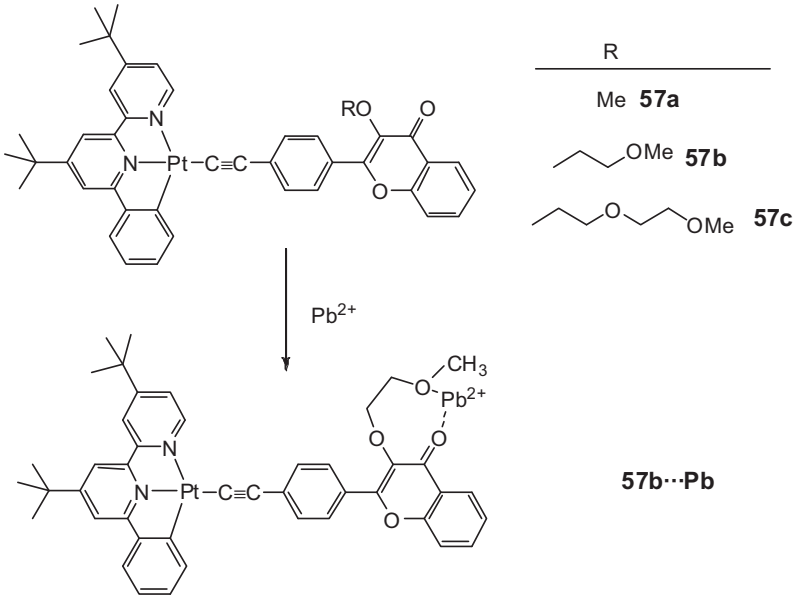

Chart 11.

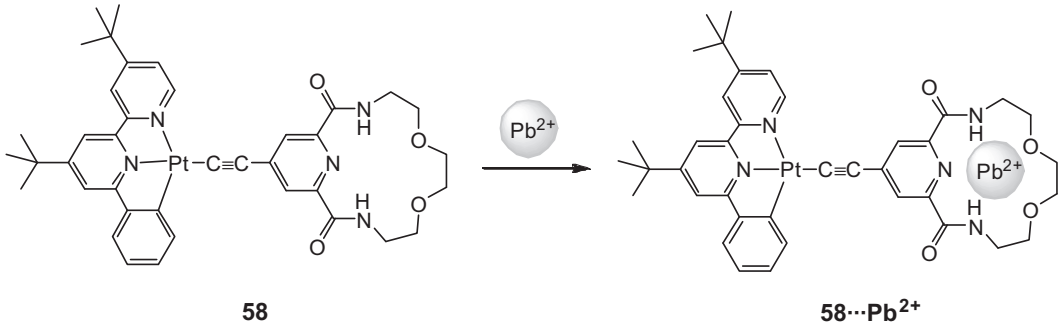

Scheme 5.

response was suggested to arise from a rare example of a switch of charge-transfer CT in the opposite direction, upon ion-binding. Thus, addition of Pb^{2+} to **58** causes a remarkable decreasing of the low MLCT/LL′CT [$d\pi(Pt) \rightarrow \pi^*(^tBu_2$-CˆNˆN)] energy manifold (370–450 nm) and the simultaneous growth of a band at 500 nm, tentatively assigned to an ML′CT [$d\pi(Pt) \rightarrow \pi^*$(C≡Cpy)] transition, with a well defined isosbestic point at 450 nm, suggestive of a ground state equilibrium between **58** and **58**···$\mathbf{Pb^{2+}}$. By complexation of Pb^{2+} ion, the intensity of emission band decreases, this being attributed to a mixed of ^{3}MLCT and ^{3}LL′CT manifold coming from the free complex **58** still present in solution. Intriguingly, by irradiation in the new absorption band (500 nm) of the complexed **58**···$\mathbf{Pb^{2+}}$, no emission was observed. It was suggested that the non-emissive ML′CT (L′ = alkynyl) state becomes the lower-lying excited state, as a result of the lower energy of the π^*(C≡Cpy) orbitals upon Pb^{2+} binding (*i.e.* a switch of CT to the opposite direction). However, it is surprising that the related pyridylacetylide platinum complex [Pt(^{t}Bu$_2$CˆNˆN)(C≡CC$_5$H$_4$N-4)] [^{t}Bu$_2$CˆNˆN = (4,4′-di*tert*-butyl)-6-phenyl-2,3′-bipyridine] did not exhibit any binding response to Pb^{2+}.

Williams and coworkers have incorporated the N-azacrown-5 and oxacrown-6 ether units shown in Chart 12 as receptors into the central 4-position of the cyclometalated NˆCˆN [1,3-di(2-pyridyl)benzene] ligand and have examined their ion-binding responses on the absorption and emission spectra [145]. The azacrown complex **59**, as the related 4-(dimethyl)aminophenyl derivative, exhibits an emission having a clear-cut intraligand charge transfer character, with the HOMO primarily localized on the pendant aminophenyl group and the LUMO on the Pt(NˆCˆN) moiety, which was suggested to change to a more stabilized TICT-like state in polar solvents (CH_2Cl_2, CH_3CN) (TICT = twisted intramolecular charge transfer). Little effect was observed for group I metal ions. However, the divalent metal ions (Mg^{2+}, Ca^{2+}, Ba^{2+}, Zn^{2+}) caused an increase in the intensity and a pronounced blue-shift in the emission in CH_3CN, the strongest effect being observed with Ca^{2+}. The changes were interpreted in terms of the inversion of the relative energies of the NˆCˆN localized and TICT excited states upon binding the Ca^{2+} to the lone pair of the azacrown nitrogen atom. In contrast, there was no change in the emission profile upon binding of metal ions to the oxacrown **60**, despite similar shifts of the lowest energy absorption to higher energies.

Following previous interest [101–103,146,147] in the design, construction and study of photophysical properties of discrete and extended self-assembled supramolecular platinum–thallium entities, Forniés, Lalinde and coworkers have examined neutralization reactions of the anionic cycloplatinated complexes (NBu$_4$)[Pt(bzq)(C≡CR)$_2$] and (NBu$_4$)[Pt(CˆN)(CN)$_2$] (CˆN = bzq, ppy) with Tl^I salts [148]. These reactions evolve with formation of sparingly soluble tetranuclear Pt_2Tl_2-based complexes [{PtTl(bzq)(C≡CR)$_2$}$_2$] (R = Ph **61**, C$_5$H$_4$N-2 **62**) and more soluble binuclear based system [PtTl(CˆN)(CN)$_2$] (CˆN = bzq **63**, ppy **64**), respectively. It is noteworthy that X-ray diffraction structures

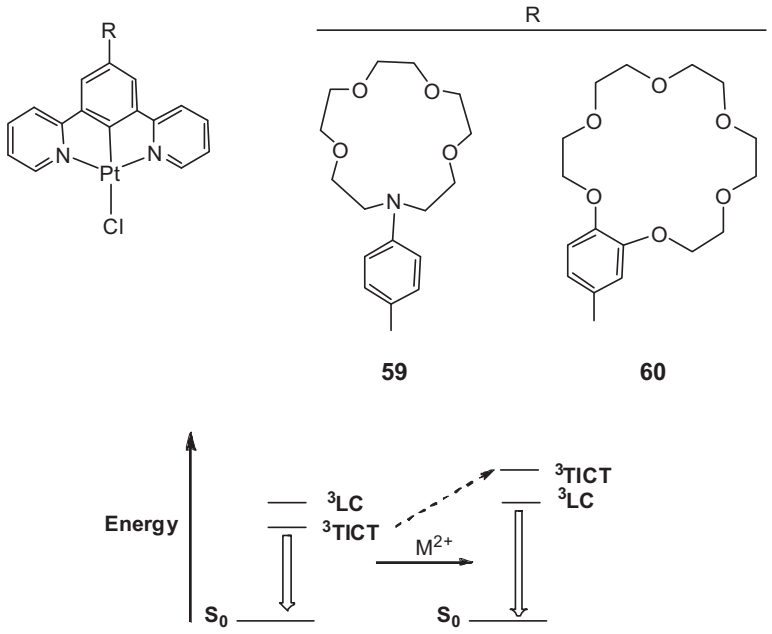

Chart 12.

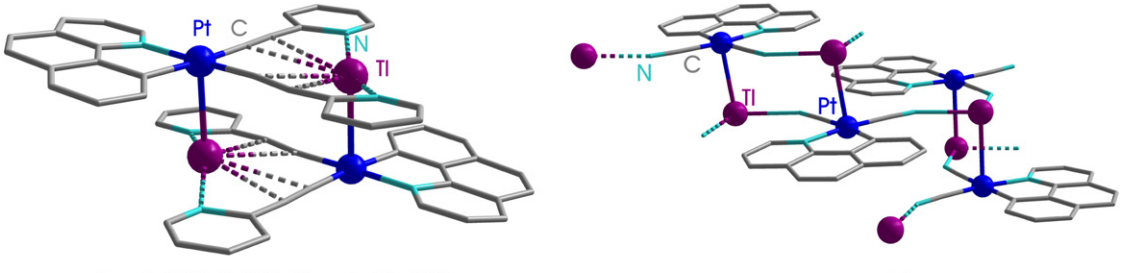

R = C_5H_4N-2 (**62**) (X-ray); Ph (**61**)

63

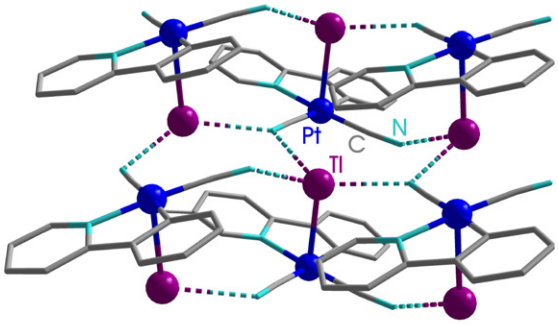

64

Chart 13.

of **62**–**64** reveal the formation, in all cases, of bimetallic fragments with a short Pt^{II}–Tl^{I} bond [2.9266(12) Å **62**, 2.9910(7) Å **63**, 3.0085(10) Å **64**], indicating a clear preference of the thallium to be bonded to the basic platinum atom. As shown in Chart 13, in complex **62**, the Pt^{II}–Tl^{I} fragment dimerizes by weak Tl···C_β(alkynyl) [3.05(2), 3.12(2) Å] and Tl···N(pyridyl) [2.85(2), 3.01(2) Å] bonding interactions, giving rise to a tetranuclear Pt_2Tl_2 entity. The solid-state packing reveals the formation of an additional network through short additional Tl···π [arene, 2-py ~ 3.45 Å] and π···π (bzq) contacts [~3.46 Å], which seems to play a role in the photophysical properties. The isoelectronic cyanide complexes **63** and **64** show extended 2-D networks generated by connection of the discrete "PtTl(CˆN)$(CN)_2$" units through two (**63**) or three (**64**) secondary Tl···N≡C contacts [2.617(8)–2.916(14) Å]. In the case of **63** containing the more delocalized benzoquinolate ligand, the layers are also associated by moderate π···π (bzq) interactions (3.6–3.8 Å). In **63**, the environment of the Tl^{I} is pyramidal, indicating a relatively strong stereo-chemical demand of the electron lone pair, and the CN^- ligands display a bent μ_2-κ*C*:κ*N* bridging mode, whereas in **64**, the Tl^{I} exhibits a distorted tetrahedral environment and the CN^- ligands show either a μ_2-κ*C*:κ*N* or the more unusual μ_3-κ*C*:κ*N*:κ*N* [103,149,150] bonding modes.

Complexes **63** and **64** are soluble in MeOH and their NMR, absorption and emission spectra are identical to those of monomer precursors, suggesting dissociation of the Pt–Tl unit. In solid state, the presence of Pt–Tl bonds and extensive π···π stacking interactions has a remarkable influence on their properties. Thus, compounds **61–63**, containing the bzq group, display an intriguing "*luminescence thermochromism*" in the solid state, which was tentatively ascribed to the presence of two low-lying emissive states. At 298 K, they show an intense low-energy (LE) broad asymmetric emission [**61**: orange, 625 nm, τ = 9.9 μs; **62**: orange-red, 640 nm, τ = 12 μs; **63**: yellow, 582 nm, τ = 2.4 μs (76%), 0.5 μs (24%)] assigned to $^3\pi\pi^*$ excimeric emission due to the occurrence of extensive π···π (bzq) interactions. Upon cooling to 77 K, the luminescence changes, and the emission is dominated by a high-energy structured (~1300 cm^{-1}) band [**61**: yellow-green, 532 nm, τ = 25.5 μs; **62**: green, 524 nm, τ = 25.4 μs; **63**: green, 512 nm, τ = 5.0 μs (30%), 50.2 μs (70%)] (Fig. 21 for **61**). In all complexes, this high emission (HE) emission is bathochromically shifted in relation to the corresponding precursors ([Pt(bzq)(C≡CR)$_2$]$^-$, R = Ph 527, 598 nm; C_5H_4N-2 508 nm; [Pt(bzq)$(CN)_2$]$^-$ 489 nm, [Pt(ppy)$(CN)_2$]$^-$ 486 nm, 77 K), a characteristic feature consistent with the formation of the Pt–Tl bond. In these systems, the good overlap between the *occupied* $5d_z^2$ and 6 s orbitals of Pt and Tl results in a bonding (σ) and an antibonding (σ*) molecular orbital, which raises the energy of the metal–metal′ [d/s σ*(Pt,Tl)] HOMO and consequently lowers the energy of the emission. This HE emission has been tentatively assigned to a metal–metal′-to-ligand (bzq) charge transfer MM′LCT [d/s σ*(Pt, Tl) → π*(bzq)] mixed, as in the corresponding precursors, with some ligand-to-ligand charge transfer (alkynyl to bzq) in complexes **61** and **62** or intraligand ^{3}LC [π(CˆN) → π*(CˆN)] in **63** and **64**. The phenylpyridinate complex **64**, which does not show *intermolecular* interactions between the

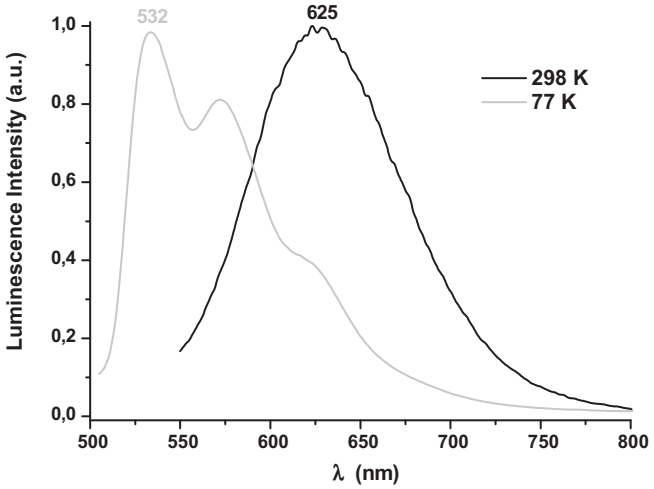

Fig. 21. Emission spectra of [{PtTl(bzq)(C≡CPh)$_2$}$_2$] **61** in solid state at 298 K and at 77 K.

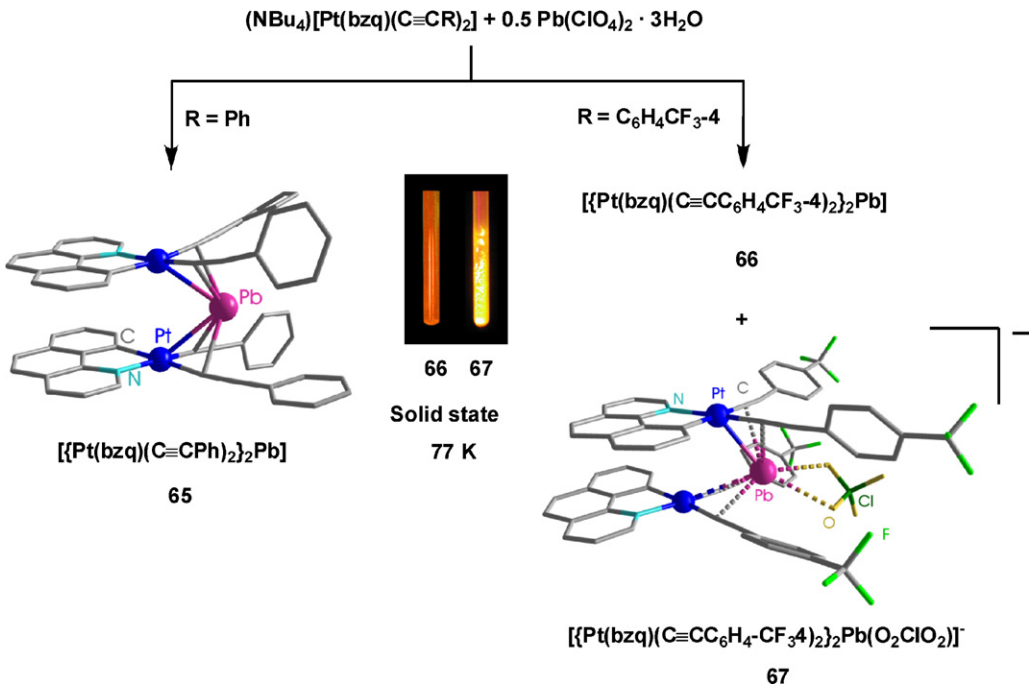

Scheme 6.

ppy groups in solid state, only exhibits the HE green structured emission both at 298 K and at 77 K, which is also bathochromically shifted in relation to that seen in the precursor (~500 nm **64** *vs.* 486 in $(NBu_4)[Pt(C^{\wedge}N)(CN)_2]$ [132]).

The ability of Pb^{II} to overlap with the Pt^{II} center has been suggested to be less effective than that of Tl^{I}. Thus, several years ago Balch and co-workers noted that in contrast to the easy formation of Pt^{II}–Tl^{I} bonds to generate $[PtTl_2(CN)_4]$ [151], the related system $K_2Pt(CN)_4/Pb(NO_3)_2$ gave the $K_2Pb[Pt(CN)_4]_2{\cdot}6H_2O$ salt, formed by zig-zag Pt···Pt bonding columns of $[Pt(CN)_4]^{2-}$ ions with the Pb^{2+} and K^+ ions set off to the side of the columns [152]. Notwithstanding, several luminescent systems containing Pt^{II}–Pb^{II} bonds, with distances widely spread, have been reported: $[(CH_3CO_2)Pb(crown\text{-}P_2)Pt(CN)_2]^+$ [152] (related to the Pt–Tl compound $[Tl(crown\text{-}P_2)Pt(CN)_2]^+$ [153]), the trinuclear linear-chain $(NBu_4)_2[\{Pt(C_6F_5)_4\}_2Pb]$ [104,154] (related to the isoelectronic $(NBu_4)_3[\{Pt(C_6F_5)_4\}_2Tl]$ [102]), $[(C_6F_5)_3Pt(\mu\text{-}X)(\mu\text{-}Pb)Pt(C_6F_5)_3]^-$ [155], the trinuclear sandwich $(NBu_4)_2[\{Pt(C{\equiv}CTol)_4\}_2Pb(OH_2)_2]$ [154] or $[Pt_2(P_2Phen)_3Pb]^{2+}$ [156].

From neutralization reactions of $(NBu_4)[Pt(bzq)(C{\equiv}CR)_2]$ (R = Ph, $C_6H_4CF_3$-4) with $Pb(ClO_4)_2$ (Scheme 6), our group has recently reported a family of novel luminescent trinuclear Pt^{II}–Pb^{II}–Pt^{II} complexes (**65**–**67**) stabilized by both Pt–Pb bonds and unusual $Pb^{II}\cdots C{\equiv}CR$ bonding interactions. It should be noted that these derivatives are the first report modelling a $Pb^{II}\cdots$alkyne bond [154], and this formation is remarkable because the related homoleptic $[Pt(C{\equiv}CTol)_4]^{2-}/Pb^{2+}$ system affords the trinuclear anionic $[\{Pt(C{\equiv}CTol)_4\}_2Pb(OH_2)_2]^{2-}$, stabilized only by Pt–Pb bonds [154].

As shown in Scheme 6, the reactions depend on the alkynyl substituent. Using the phenylethynyl derivative, the neutral trinuclear sandwich-type complex **65** is generated, which is formed by two eclipsed and very close platinate fragments [intramolecular contacts Pt···Pt 3.5794(5) Å, bzq···bzq 3.36–3.48 Å] connected by a lead center [154].

The Pb^{II} center shows a symmetric *hemidirected* coordination, being bonded to the four Pt–C_α bonds [Pt–Pb 2.9759(5), 2.9182(5) Å; Pb–C_α 2.619(9)–2.682(9) Å], which define the basal plane of a square pyramidal geometry, and has the $6s^2$ lone pair at the apex of the pyramid. The crystal packing reveals that the Pt_2Pb clusters self-assemble in a head-to-tail orientation by intermolecular π···π(bzq) bonding interactions [3.36–3.42 Å] forming stacking dimers, a feature that also has influence on its optical properties. Conductivity measurements, NMR and electronic spectra indicate that the trinuclear entity remains in solution. In fact, its UV–vis spectrum exhibits a low-energy feature at 430 nm, absent in the platinum monomer (λ_{max} 397 nm) attributed, as in related heteropolymetal η-alkynyl bridging complexes, to admixture of platinum perturbed intraligand [$\pi \rightarrow \pi^*(C{\equiv}CPh)$] and LM′CT [alkynyl or platinum-alkynyl → M′(Pb)] charge transfer [$Pt(C{\equiv}CPh) \rightarrow 6s/p(Pb)$]. This cluster (**65**) shows a bright yellow emission (575 nm) in diluted (5×10^{-5} M) CH_2Cl_2 solution, which has been tentatively assigned to a ^{3}MLM′CT [$Pt(d)/\pi(C{\equiv}CPh) \rightarrow Pt(p_z)/Pb(sp)/\pi^*(C{\equiv}CPh)$] state, modified by metal···metal interactions in view of the short Pt···Pb and Pt···Pt [3.5794(5) Å] distances. Intriguingly, this emission is quenched by increasing concentration to 10^{-3} M, and also in the solid state at 298 K, probably because of the formation of dimers through intermolecular π···π(bzq) interactions, as found in the solid lattice. Upon cooling the solid to 77 K, the quenching seems to be less effective and **65** exhibits a bright long lived (24 μs) orange emission (607 nm), tentatively assigned to a ^{3}MLM′CT excited state probably combined with some ππ* excimeric character.

However, the analogous system $[Pt(bzq)(C{\equiv}C\text{-}C_6H_4CF_3\text{-}4)_2]^-/Pb(ClO_4)_2$ (2:1), containing the less electron-donating $C_6H_4CF_3$-4 alkynyl substituent, originates the related neutral Pt_2Pb cluster **66** as an orange solid in a low yield (8.5%) together with the new perchlorate adduct $(NBu_4)[\{Pt(bzq)(C{\equiv}C\text{-}C_6H_4CF_3\text{-}4)_2\}_2Pb(O_2ClO_2)]$ **67**, as a yellow microcrystalline solid (~40%). In the anion **67**$^-$, the platinum fragments are displaced and, probably due to the electron-poor nature of the $C_6H_4CF_3$-4 alkynyl substituents, the interaction of the Pb^{II} with the platinum and the C_α alkynyl atoms is asymmetric and weaker [Pt–Pb 2.8715(5), 3.3136(5) Å; Pb–C_α 2.630(9)–2.772(10) Å] to that seen in **65**. As a consequence, the acidic Pb^{II} completes a more complicated environment by a weak contact with the perchlorate anion [Pb–O 2.880(8), 3.013(8) Å] in an asymmetrical chelating way.

Complexes **66** and **67** are strongly emissive only in the solid state at 77 K, with emission bands red-shifted (620, 660sh **66**, 600 nm **67**) in relation to **65**, assigned to a similar ^{3}MLM′CT excited state, probably combined with some $\pi\pi^*$ excimeric character in **66**. The decrease in the energy gap of the emission is in agreement with the involvement of the lower lying π^*(C≡C–$C_6H_4CF_3$-4) orbitals, which are better accepting than π^*(C≡CPh) in **65**. In the adduct **67**, the significant shift to high energies observed in relation to neutral cluster **66** (600 nm **67** *vs*. 620 nm **66**) could be apparently caused by the presence of Pb···O ($O_2ClO_2^-$) contacts, which presumably weaken the interaction of the Pb^{II} center with the C≡C–$C_6H_4CF_3$-4 units, thus increasing the energy of the π^*(C≡CAryl) based LUMO. For **66** and **67**, conductivity and NMR measurements indicate considerable dissociation in solution, and they do not exhibit luminescence in CH_2Cl_2 at 298 K. In rigid glass (77 K), **67** showed a dual emission (575 and 660 nm) derived from the presence of different emissive species (including **66**).

Recently, a new series of highly efficient phosphorescent [Pt(ppy-X)(acac)] complexes with different electronic main group moieties substituted at the *para* position in the 2-phenylpyridinate have been reported [157], which exhibited improved properties in OLEDs and WOLEDs devices. Among these, the devices made from the Pt–Ge (X = $GePh_3$) emitter (green due to monomer and orange/red from aggregate excimer) adequately combined with the intrinsic properties of the blue-emitting hole-transport NPB (4,4′-bis[*N*-1-napththyl)-*N*-phenylamino]biphenyl) achieved single-dopant WOLEDs, which emits white light of very high quality.

5. Conclusions and perspectives

Cycloplatinated complexes have been demonstrated to be useful building blocks in the design of heteropolynuclear and/or multicomponent architectures. Easy access to heteropolymetallic cycloplatinated systems has been described but only in few cases have the photoluminescence properties been studied. In terms of emitters, we believe the following to be of particular interest:

i) The possibility of linking a chromophore cycloplatinate unit to a distinct d^6 emitter, as in the Pt^{II}–Ir^{III} complex linked by a bis(β-diketonato) bridging ligand (**9**), which opens up a field to be explored.
ii) The growing family of Pt^{II}–M complexes (M = d^{10} Ag^I, Cu^I, Cd^{II}; s^2 Tl^I, Pb^{II}) with Pt–M bonds (unsupported or in cooperation with bridging ligands), which show interesting structures and photophysical properties. The observation of substantial blue- or red-shifts (absorption and emission) upon formation of dative Pt–M (d^{10}) and Pt–Tl bonds, respectively, as well as the occurrence of polymorphism and its influence on the photophysical properties of the sandwich anion $[\{Pt(bzq)(C_6F_5)_2\}_2Ag]^-$ (**21**) indicate that this type of systems offer a different approach to modifying the emission of cycloplatinated chromophores. The incorporation of auxiliary ligands such as alkynyl or cyanide groups, with versatile bonding modes, clearly expands the possibility for research in this field, leading to heteropolynuclear aggregates with interesting spectroscopic properties, including vapochromism or multiple emissions coming from close emissive manifolds.
iii) The behavior of some cycloplatinate-based systems as effective sensors of metal ions, in some cases in selective way, by incorporating adequate receptors either on the coligands (*i.e.* functionalised acetylide groups) or on the cyclometalated group. Finally, considerable attention is due to the construction of peripherally cyclometalated porphyrin or diporphyrin architectures obtained through studied cyclometalation strategies.

The exceptional bright luminescence of heteropolynuclear cycloplatinated complexes is exciting, although the potential of this type of systems has scarcely begun to be explored. As expected, not only the nature of the heterometal but also the configuration of the cyclometalated group and/or the coligands exert a great effect on the structure and phosphorescent characteristics of the final organometallic product.

In summary, this is a promising field and the results shown in this work would encourage further research in this area. As the range of heteropolynuclear complexes with luminescent properties expands, extensive applications should arise at the same time in OLEDs, sensors, light-emitting devices or other molecular optoelectronic applications.

Acknowledgments

This work was supported by the Spanish MICINN (Project CTQ2008-06669-C02-02/BQU and a grant for A. Díez). Authors thank all their co-workers involved in cycloplatinated systems for their dedication and to Prof. Dr. Juan Forniés and his research group for his continuous scientific and personal support.

References

[1] J.A.G. Williams, Top. Curr. Chem. 281 (2007) 205.
[2] J.A.G. Williams, S. Develay, D.L. Rochester, L. Murphy, Coord. Chem. Rev. 252 (2008) 2596.
[3] J.A.G. Williams, Chem. Soc. Rev. 38 (2009) 1783.
[4] R. McGuire Jr., M.C. McGuire, D.R. McMillin, Coord. Chem. Rev. 254 (2010) 2574.
[5] Y. Chi, P.T. Chou, Chem. Soc. Rev. 39 (2010) 638.
[6] B. Ma, P.I. Djurovich, M.E. Thompson, Coord. Chem. Rev. 249 (2005) 1501.
[7] H. Yersin, D. Donges, Top. Curr. Chem. 214 (2001) 81.
[8] S.W. Lai, C.M. Che, Top. Curr. Chem. 241 (2004) 27.
[9] A.F. Rausch, H.H.H. Homeier, H. Yersin, Top. Organomet. Chem. 29 (2010) 193.
[10] L. Murphy, J.A.G. Williams, Top. Organomet. Chem. 28 (2010) 75.
[11] R.C. Evans, P. Douglas, C. Winscom, Coord. Chem. Rev. 250 (2006) 2093.
[12] H.F. Xiang, S.W. Lai, P.T. Lai, C.M. Che, in: H. Yersin (Ed.), Highly Efficient OLEDs with Phosphorescent Materials, Wiley-VCH, Weinheim, Germany, 2007.
[13] C. Yang, X. Zhang, H. You, L. Zhu, L. Chen, L. Zhu, Y. Tao, D. Ma, Z. Shuai, J. Quin, Adv. Funct. Mater. 17 (2007) 651.
[14] M. Cocchi, D. Virgili, V. Fattori, D.L. Rochester, J.A.G. Williams, Adv. Funct. Mater. 17 (2007) 285.
[15] N.M. Shavaleev, H. Adams, J. Best, R. Edge, S. Navaratnam, J. Weinstein, Inorg. Chem. 45 (2006) 9410.
[16] C.K. Koo, L.K.Y. So, K.L. Wong, Y.M. Ho, Y.W. Lam, M.H.W. Lam, K.W. Cheah, C.C.W. Cheng, W.M. Kwok, Chem. Eur. J. 16 (2010) 3942.
[17] V.W.W. Yam, R.P.L. Tang, K.M.C. Wong, X.X. Lu, K.K. Cheung, N. Zhu, Chem. Eur. J. 8 (2002) 4066.
[18] D.L. Ma, C.M. Che, S.C. Yan, J. Am. Chem. Soc. 131 (2009) 1835.
[19] P. Wu, E.L.M. Wong, D.L. Ma, G.S.M. Tong, K.M. Ng, C.M. Che, Chem. Eur. J. 15 (2009) 3652.
[20] M. Kato, Bull. Chem. Soc. Jpn. 80 (2007) 287.
[21] D.M. Roundhill, H.B. Gray, C.M. Che, Acc. Chem. Res. 22 (1989) 55.
[22] V.M. Miskowski, V.H. Houlding, Inorg. Chem. 30 (1991) 4446.
[23] J. Schneider, P. Du, P. Jarosz, T. Lazarides, X. Wang, W.W. Brennessel, R. Eisenberg, Inorg. Chem. 48 (2009) 4306.
[24] W. Lu, M.C.W. Chan, K.K. Cheung, C.M. Che, Organometallics 20 (2001) 2477.
[25] A. Díez, J. Forniés, C. Larraz, E. Lalinde, J.A. López, A. Martín, M.T. Moreno, V. Sicilia, Inorg. Chem. 49 (2010) 3239.
[26] M.Y. Yuen, V.A.L. Roy, W. Lu, S.C.F. Kui, G.S.M. Tong, M.H. So, S.S.Y. Chui, M. Muccini, J.Q. Ning, S.J. Xu, C.M. Che, Angew. Chem. Int. Ed. 47 (2008) 9895.
[27] W. Lu, S.S.Y. Chui, K.M. Ng, C.M. Che, Angew. Chem. Int. Ed. 47 (2008) 4568.
[28] D. Kim, J.L. Brédas, J. Am. Chem. Soc. 131 (2009) 11371.
[29] Y. Chen, K. Li, W. Lu, S.S.Y. Chui, C.W. Ma, C.M. Che, Angew. Chem. Int. Ed. 48 (2009) 9909.
[30] W. Lu, V.A.L. Roy, C.M. Che, Chem. Commun. (2006) 3972.
[31] S.C.F. Kui, S.S.Y. Chui, C.M. Che, N. Zhu, J. Am. Chem. Soc. 128 (2006) 8297.
[32] A.A. Rachford, F.N. Castellano, Inorg. Chem. 48 (2009) 10865.
[33] B. Ma, J. Li, P.I. Djurovich, M. Yousufuddin, R. Bau, M.E. Thompson, J. Am. Chem. Soc. 127 (2005) 28.
[34] W. Lu, M.C.W. Chan, N. Zhu, C.M. Che, C. Li, Z. Hui, J. Am. Chem. Soc. 126 (2004) 7639.
[35] W. Sun, H. Zhu, P.M. Barron, Chem. Matter 18 (2006) 2602.
[36] J. Hu, R. Lin, J.H.K. Yip, K.Y. Wong, D.L. Ma, J.J. Vittal, Organometallics 26 (2007) 6533.
[37] S.C.F. Kui, I.H.T. Sham, C.C.C. Cheung, C.W. Ma, B. Yan, N. Zhu, C.M. Che, W.F. Fu, Chem. Eur. J. 13 (2007) 417.
[38] P. Shao, W. Sun, Inorg. Chem. 46 (2007) 8603.

[39] J. Ding, D. Pan, C.H. Tung, L.Z. Wu, Inorg. Chem. 47 (2008) 5099.
[40] H. Jude, J.A.K. Bauer, W.B. Connick, Inorg. Chem. 44 (2005) 1211.
[41] B. Ma, P.I. Djurovich, M. Yousufuddin, R. Bau, M.E. Thompson, J. Phys. Chem. C 112 (2008) 8022.
[42] T. Koshiyama, A. Omura, M. Kato, Chem. Lett. 33 (2004) 1386.
[43] P. Shao, Y. Li, A. Azenkeng, M.R. Hoffmann, W. Sun, Inorg. Chem. 48 (2009) 2407.
[44] Z. Guo, M.C.W. Chan, Chem. Eur. J. 15 (2009) 12585.
[45] B. Ma, P.I. Djurovich, S. Garon, B. Allyne, M.E. Thompson, Adv. Funct. Mater. 16 (2006) 2438.
[46] I. Eryazici, C.N. Moorefield, G.R. Newkome, Chem. Rev. 108 (2008) 1834.
[47] S.D. Cummings, Coord. Chem. Rev. 253 (2009) 449.
[48] K.M.C. Wong, V.W.W. Yam, Coord. Chem. Rev. 251 (2007) 2477.
[49] F.N. Castellano, I.E. Pomestchenko, E. Shikhova, F. Hua, M.L. Muro, N. Rajapakse, Coord. Chem. Rev. 250 (2006) 1819.
[50] J. van Slageren, A. Klein, S. Záliš, Coord. Chem. Rev. 230 (2002) 193.
[51] M. Hissler, J.E. McGarrah, W.B. Connick, D.K. Geiger, S.D. Cummings, R. Eisenberg, Coord. Chem. Rev. 208 (2000) 115.
[52] R. Ziessel, M. Hissler, A. El-ghayoury, A. Harriman, Coord. Chem. Rev. 178–180 (1998) 1251.
[53] Z.N. Chen, N. Zhao, Y. Fan, J. Ni, Coord. Chem. Rev. 253 (2009) 1.
[54] Z.N. Chen, Y. Fan, J. Ni, Dalton Trans. (2008) 573.
[55] J.R. Berenguer, E. Lalinde, M.T. Moreno, Coord. Chem. Rev. 254 (2010) 832.
[56] K.M.C. Wong, C.K. Hui, K.L. Yu, V.W.W. Yam, Coord. Chem. Rev. 229 (2002) 123.
[57] E.J. Fernández, A. Laguna, J.M. López-de-Luzuriaga, Dalton Trans. (2007) 1969.
[58] V.W.W. Yam, E.C.C. Cheng, Chem. Soc. Rev. 37 (2008) 1806.
[59] P. Pykkö, Chem. Rev. 97 (1997) 597.
[60] C.M. Che, S.W. Lai, Coord. Chem. Rev. 249 (2005) 1296.
[61] V.W.W. Yam, K.K.W. Lo, K.M.C. Wong, J. Organomet. Chem. 578 (1999) 3.
[62] J.M. Forward, J.P.J. Fackler, Z. Assefa, in: D.M. Roundhill, J.P. Fackler Jr. (Eds.), Optoelectronic Properties of Inorganic Compounds, Plenum Press, New York, 1999, p. 195.
[63] M.J. Katz, K. Sakai, D.B. Leznoff, Chem. Soc. Rev. 37 (2008) 1884.
[64] C. Mealli, F. Pichierri, L. Randaccio, E. Zangrando, M. Krumm, D. Holtenrich, B. Lippert, Inorg. Chem. 34 (1995) 3418.
[65] G. Aullón, S. Alvarez, Inorg. Chem. 35 (1996) 3137.
[66] Y. Wu, S. Huo, J. Gong, X. Cui, L. Ding, K. Ding, C. Du, Y. Liu, M. Song, J. Organomet. Chem. 637–639 (2001) 27.
[67] Y. Wu, L. Ding, H.X. Wang, H. Liu, H.Z. Yuan, X.A. Mao, J. Organomet. Chem. 535 (1997) 49.
[68] A.D. Ryabov, G.M. Kazankov, J.M. Payashkina, O.V. Grozovsky, O.G. Dyavhenko, V.A. Polyakov, L.G. Kuz'mina, J. Chem. Soc., Dalton Trans. (1997) 4385.
[69] A.D. Ryabov, J.M. Payashkina, V.A. Polyakov, J.A.K. Howard, L.G. Kuz'mina, M.S. Dott, S. Sacht, Organometallics 17 (1998) 3615.
[70] C.J. McAdam, E.J. Blackie, J.L. Morgan, S.A. Mole, B.H. Robinson, J. Simpson, Dalton Trans. (2001) 2362.
[71] P.R.R. Ranatunge-Bandarage, B.H. Robinson, J. Simpson, Organometallics 14 (1994) 500.
[72] P.R.R. Ranatunge-Bandarage, N.N. Duffy, S.J. Johnson, J. Simpson, Organometallics 13 (1994) 511.
[73] S. Pérez, C. López, A. Caubet, X. Solans, M. Font-Bardía, New J. Chem. 27 (2003) 975.
[74] S. Pérez, C. López, A. Caubet, X. Solans, M. Font-Bardia, J. Organomet. Chem. 689 (2004) 3184.
[75] C. López, X. Solans, M. Font-Bardía, Inorg. Chem. Commun. 8 (2005) 631.
[76] S. Pérez, C. López, A. Caubet, R. Bosque, X. Solans, M. Font-Bardía, A. Roig, E. Molins, Organometallics 23 (2004) 224.
[77] R. Packheiser, P. Ecorchard, B. Walfort, H. Lang, J. Organomet. Chem. 693 (2008) 933.
[78] S. Back, R.A. Gossage, H. Lang, G. van Koten, Eur. J. Inorg. Chem. (2000) 1457.
[79] S. Back, R.A. Gossage, M. Lutz, I. del Río, A.L. Spek, H. Lang, G. van Koten, Organometallics 19 (2000) 3296.
[80] S. Jamali, S.M. Nabavizadeh, M. Rashidi, Inorg. Chem. 47 (2008) 5441.
[81] C.H. Shin, J.O. Huh, S.J. Baek, S.K. Kim, M.H. Lee, Y. Do, Eur. J. Inorg. Chem. (2010) 3642.
[82] J. Forniés, S. Fuertes, A. Martín, V. Sicilia, E. Lalinde, M.T. Moreno, Chem. Eur. J. 12 (2006) 8253.
[83] P. Steenwinkel, S.L. James, D.M. Grove, H. Kooijman, A.L. Spek, G. van Koten, Organometallics 16 (2007) 513.
[84] S. Yamaguchi, H. Shinokubo, A. Osuka, Inorg. Chem. 48 (2009) 795.
[85] S. Yamaguchi, T. Katoh, H. Shinokubo, A. Osuka, J. Am. Chem. Soc. 130 (2008) 14440.
[86] P.J. Chmielewski, I. Schmidt, Inorg. Chem. 43 (2004) 1885.
[87] J. Forniés, A. Martín, in: P. Braunstein, L.A. Oro, P.R. Raithby (Eds.), Metal Clusters in Chemistry, 1999, Wiley-VCH, New York, 1999, p. 417.
[88] J.R. Stork, D. Rios, D. Pham, V. Bicocca, M.M. Olmstead, A.L. Balch, Inorg. Chem. 44 (2005) 3466.
[89] F. Liu, W. Chen, D. Wang, Dalton Trans. (2006) 3015.
[90] M. Stender, R.L. White-Morris, M.M. Olmstead, A.L. Balch, Inorg. Chem. 42 (2003) 4504.
[91] B.H. Xia, H.X. Zhang, C.M. Che, K.H. Leung, D.L. Phillips, N. Zhu, Z.Y. Zhou, J. Am. Chem. Soc. 125 (2003) 10362.
[92] G.Q. Yin, Q.H. Wei, L.Y. Zhang, Z.N. Chen, Organometallics 25 (2006) 580.
[93] Q.H. Wei, G.Q. Yin, Z. Ma, L.X. Shi, Z.N. Chen, Chem. Commun. (2003) 2188.
[94] Y.D. Chen, L.Y. Zhang, L.X. Shi, Z.N. Chen, Inorg. Chem. 43 (2004) 7493.
[95] T.R. Cook, A.J. Esswein, D.G. Nocera, J. Am. Chem. Soc. 129 (2007) 10094.
[96] K. Umakoshi, T. Kojima, K. Saito, S. Akatsu, M. Onishi, S. Ishizaka, N. Kitamura, Y. Nakao, S. Sakaki, Y. Ozaura, Inorg. Chem. 47 (2008) 5033.
[97] L.R. Falvello, J. Forniés, E. Lalinde, B. Menjón, M.A. García-Monforte, M.T. Moreno, M. Tomás, Chem. Commun. (2007) 3838.
[98] T. Yamaguchi, F. Yamazaki, T. Ito, J. Am. Chem. Soc. 123 (2001) 743.
[99] D.E. Janzen, L.F. Mehne, D.G. van Derveer, G.J. Grant, Inorg. Chem. 44 (2005) 8182.
[100] J. Forniés, S. Ibáñez, A. Martín, M. Sanz, J.R. Berenguer, E. Lalinde, J. Torroba, Organometallics 25 (2006) 4331.
[101] J.P.H. Charmant, J. Forniés, J. Gómez, E. Lalinde, R.I. Merino, M.T. Moreno, A.G. Orpen, Organometallics 22 (2003) 652.
[102] L.R. Falvello, J. Forniés, R. Garde, A. García, E. Lalinde, M.T. Moreno, A. Steiner, M. Tomás, I. Usón, Inorg. Chem. 45 (2006) 2543.
[103] J. Forniés, A. García, E. Lalinde, M.T. Moreno, Inorg. Chem. 47 (2008) 3651.
[104] R. Usón, J. Forniés, L.R. Falvello, M.A. Usón, I. Usón, Inorg. Chem. 31 (1992) 3697.
[105] R. Usón, J. Forniés, M. Tomás, I. Usón, Angew. Chem. Int. Ed. 29 (1990) 1449.
[106] Q. Zhao, L. Li, F. Li, M. Yu, Z. Liu, T. Yi, C. Huang, Chem. Commun. (2008) 685.
[107] Y. You, H.S. Huh, K.S. Kim, S.W. Lee, D. Kim, S.Y. Park, Chem. Commun. (2008) 3998.
[108] K. Huang, H. Wu, M. Shi, F. Li, T. Yi, C. Huang, Chem. Commun. (2009) 1243.
[109] I. Mathew, W. Sun, Dalton Trans. (2010) 5885.
[110] K.H.Y. Chan, J.W.Y. Lam, K.M.C. Wong, B.Z. Tang, V.W.W. Yam, Chem. Eur. J. 15 (2009) 2328.
[111] M.X. Zhu, W. Lu, N. Zhu, C.M. Che, Chem. Eur. J. 14 (2008) 9736.
[112] C. Yu, K.H.Y. Chan, K.M.C. Wong, V.W.W. Yam, Chem. Eur. J. 14 (2008) 4577.
[113] V.W.W. Yam, K.H.Y. Chan, K.M.C. Wong, N. Zhu, Chem. Eur. J. 11 (2005) 4535.
[114] S. Jamali, Z. Mazloomi, S.M. Nabavizadeh, D. Milli'c, R. Kia, M. Rashidi, Inorg. Chem. 49 (2010) 2721.
[115] $[Pt_2(C^{\wedge}P)_2(S_2CNMe_2)_2Ag\{Ag(OClO_3)\}]ClO_4$ **27** crystallizes as a mixture of **27**$^+$ and **27**$\{OH_2\}^+$ in 1:1 molar ratio.
[116] J. Forniés, A. Martín, R. Navarro, V. Sicilia, P. Villarroya, A.G. Orpen, J. Chem. Soc., Dalton Trans. (1998) 3721.
[117] L.R. Falvello, J. Forniés, A. Martín, V. Sicilia, P. Villarroya, Organometallics 21 (2002) 4604.
[118] J.M. Casas, J. Forniés, S. Fuertes, A. Martín, V. Sicilia, Organometallics 26 (2007) 1674.
[119] A. Díez, A. García, E. Lalinde, M.T. Moreno, Eur. J. Inorg. Chem. (2009) 3060.
[120] A. Díez, PhD Doctoral Thesis; Universidad de La Rioja, 2010.
[121] A. Díez, A. García, J. Forniés, E. Lalinde, M.T. Moreno, Unusual clusters-based chains and study of their optical properties, in: 9th FIGIPAS Meeting in Inorganic Chemisty, Vienna, Austria, 2007.
[122] L.R. Falvello, J. Forniés, A. Martín, R. Navarro, V. Sicilia, P. Villarroya, Inorg. Chem. 36 (1997) 6166.
[123] J. Forniés, A. Martín, V. Sicilia, P. Villarroya, Organometallics 19 (2000) 1107.
[124] I. Ara, L.R. Falvello, J. Forniés, V. Sicilia, P. Villarroya, Organometallics 19 (2000) 3091.
[125] I. Ara, J. Forniés, V. Sicilia, P. Villarroya, Dalton Trans. (2003) 4238.
[126] M.A. Bennett, M. Contel, D.C.R. Hockless, L.L. Welling, A.C. Willis, Inorg. Chem. 41 (2002) 844.
[127] A.F.M.J. van der Ploeg, G. van Koten, K. Vrieze, A.L. Spek, Inorg. Chem. 21 (1982) 2014.
[128] A.F.M.J. van der Ploeg, G. van Koten, K. Vrieze, A.L. Spek, A.J.M. Duisenberg, Organometallics 1 (1982) 1066.
[129] T. Yamaguchi, F. Yamazaki, T. Ito, J. Am. Chem. Soc. 121 (1999) 7405.
[130] J. Forniés, S. Ibáñez, A. Martín, B. Gil, E. Lalinde, M.T. Moreno, Organometallics 23 (2004) 3963.
[131] Q.Y. Cao, X. Gan, J.F. Zhang, S.M. Chi, H.F. Li, W.F. Fu, Chin. J. Chem. 25 (2007) 1821.
[132] J. Forniés, S. Fuertes, J.A. López, A. Martín, V. Sicilia, Inorg. Chem. 47 (2008) 7166.
[133] M. Kobayashi, S. Masaoka, K. Sakai, Photochem. Photobiol. Sci. 8 (2009) 196.
[134] D. Song, R.H. Morris, Organometallics 23 (2004) 4406.
[135] Y. Fan, Y.M. Zhu, F.R. Dai, L.Y. Zahang, Z.N. Chen, Dalton Trans. (2007) 3885.
[136] W.S. Tang, X.X. Lu, K.M.C. Wong, V.W.W. Yam, J. Mater. Chem. 15 (2005) 2714.
[137] K.M.C. Wong, W.S. Tang, X.X. Lu, N. Zhu, V.W.W. Yam, Inorg. Chem. 44 (2005) 1492.
[138] X. Han, L.Z. Wu, G. Si, J. Pan, Q.Z. Yang, L.P. Zhang, C.H. Tung, Chem. Eur. J. 13 (2007) 1231.
[139] V.W.W. Yam, R.P.L. Tang, K.M.C. Wong, K.K. Cheung, Organometallics 20 (2001) 4476.
[140] Z. Ji, Y. Li, W. Sun, Inorg. Chem. 47 (2008) 7599.
[141] Q.Z. Yang, Q.X. Tong, L.Z. Wu, Z.X. Wu, L.P. Zhang, C.H. Tung, Eur. J. Inorg. Chem. (2004) 1948.
[142] Q.Z. Yang, L.Z. Wu, H. Zhang, B. Chen, Z.X. Wu, L.P. Zhang, C.H. Tung, Inorg. Chem. 43 (2004) 5195.
[143] P.H. Lanoë, J.L. Fillaut, L. Toupet, J.A.G. Williams, H.L. Bozec, V. Guerchais, Chem. Commun. (2008) 4333.
[144] P.H. Lanoë, H. Le Bozec, J.A.G. Williams, J.L. Fillaut, V. Guerchais, Dalton Trans. 39 (2010) 707.
[145] D.L. Rochester, S. Develay, S. Záliš, J.A.G. Williams, Dalton Trans. (2009) 1728.
[146] J.R. Berenguer, J. Forniés, J. Gómez, E. Lalinde, M.T. Moreno, Organometallics 20 (2001) 4847.
[147] J.R. Berenguer, J. Forniés, B. Gil, E. Lalinde, Chem. Eur. J. 12 (2006) 785.

[148] J. Forniés, S. Fuertes, A. Martín, V. Sicilia, B. Gil, E. Lalinde, Dalton Trans. (2009) 2224.
[149] N.G. Connelly, O.M. Hicks, G.R. Lewis, M.T. Moreno, A.G. Orpen, J. Chem. Soc., Dalton Trans. (1998) 1913.
[150] C. Eaborn, M.S. Hill, P.B. Hitchcok, J.D. Smith, Organometallics 19 (2000) 5780.
[151] J.K. Nagle, A.L. Balch, M.M. Olmstead, J. Am. Chem. Soc. 110 (1988) 319.
[152] A.L. Balch, E.Y. Fung, J.K. Nagle, M.M. Olmstead, S.P. Rowley, Inorg. Chem. 32 (1993) 3295.
[153] A.L. Balch, S.P. Rowley, J. Am. Chem. Soc. 112 (1990) 6139.
[154] J.R. Berenguer, A. Díez, J. Fernández, J. Forniés, A. García, B. Gil, E. Lalinde, M.T. Moreno, Inorg. Chem. 47 (2008) 7703.
[155] J.M. Casas, J. Forniés, A. Martín, V.M. Orera, A.G. Orpen, A. Rueda, Inorg. Chem. 34 (1995) 6514.
[156] V.J. Catalano, B.L. Bennett, B.C. Noll, Chem. Commun. (2000) 1413.
[157] G. Zhou, Q. Wang, X. Wang, C.L. Ho, W.Y. Wong, D. Ma, L. Wang, Z. Lin, J. Mater. Chem. 20 (2010) 7472.